Co-financed by the EC
DIRECTORATE-GENERAL HUMANITARIAN AID AND CIVIL PROTECTION – ECHO

AGREEMENT NUMBER - ECHO/SUB/2015/718655/PREV28

KnowRISK

Know your city, Reduce seISmic risK through non-structural elements

Prevention and preparedness projects in civil protection and marine pollution. Prevention Priorities

Deliverable Report

Deliverable B1 – Definition of seismic scenarios

Task B – RiskMAP

Deliverable/Task Leader: IST, INGV

March, 2018

Project co-funded by the European Commission – Civil Protection Financial Instrument		
Dissemination Level		
PU	Public	x
PP	Restricted to other programme participants (including the Commission Services)	
RE	Restricted to a group specified by the consortium (including the Commission Services)	
CO	Confidential, only for members of the consortium (including the Commission Services)	

TABLE OF CONTENTS

LIST OF FIGURES

LIST OF SYMBOLS AND ABBREVIATIONS

SISZ	South Iceland Seismic Zone
MR	Mid-Atlantic Ridge
TFZ	Tjörnes Fracture Zone
WVZ	Western Volcanic Zone
EVZ	Eastern Volcanic Zone
Mw	Moment Magnitude
MMI	Modified Mercalli Intensity

1. DESCRIPTION OF THE DELIVERABLE

1.1 INTRODUCTION

This action aims at producing seismic scenarios focused on non-structural damage in pilot areas of the three participating countries, namely i) Lisbon in Portugal, ii) Etna and Northern Regions in Italy, and iii) the South Iceland Seismic Zone. In methodological terms, the hazard analysis considers macroseismic data together with other ground motion parameters instrumentally derived or by means of synthetic simulations. This action is addressed to map the areas that are mostly exposed to intensities/shaking typically representative of non-structural damage.

1.2 SEISMIC SCENARIOS FOR LISBON PILOT AREA

1.2.1. Introduction

Portugal is a country considered as with a moderate seismicity, however with some peculiarities. In what respects to Lisbon, it seems that a pattern characterized by two kind of ground shaking intensities seems to exist. One, with Inter-Arrival Times (IAT or Return Periods, TR) of around 90-150 years leading to Intensities of about 6,5 – 7,5, and another one, with a larger TR of about 200-250 years with higher values of ground shaking, leading to Intensities of 8,0 – 9,0 in the 1998 European Macroseismic Scale (EMSS). Besides that, earthquakes in Portugal have their genesis in seismogenic regions with different characteristics: Inter-Plate sources located offshore, in the South, generated in the junction of the Euro-Asian and in the African Plates, and Intra-Plates onshore faults acting as near-sources, with higher frequency contents. It can be noticed by the historical records that both mixes of Magnitude-Distance and Earthquake Type (I or II) can be responsible by the two Damages Clusters (Moderate Intensities prone to high Non-Structural Losses, and High Intensities responsible by high Structural losses, where in this last case Non-Structural Lossescur become less important. In both cases, the dimension of the seismogenic regions is large enough to lead to a high uncertainty about plausible epicenter locations, and so a high uncertainty in epicentral distances to the targeted cities or regions.

During this Action B1.1 several tasks were performed and completed:

1. Portuguese Seismic Hazard was reviewed, with special emphasis to the City of Lisbon,

2. Portuguese Building Stock was also reviewed and adapted in order to feed the most recent Seismic Simulator and Damages Models. This resulted in a data-base with about 16.647.423 records to the 255.897 Urban Blocks in Portugal Mainland, and, for each one of them the number of buildings from each of the 69 typologies. For the case of Lisbon, this resulted in a Database with 33.730 georeferenced records, covering the whole Lisbon Building Stock.

3. Data was organized and prepared in GeoData (GIS) Format, in order to feed the QuakeIST Seismic Simulator, which is now totally ready to simulate any desired scenario for Action B3. Besides that, a “Reference Scenario” designed specifically for the KnowRISKProject was here advocated, proposed and prepared.

4. The QuakeIST Seismic Simulator, was also modified in order to accommodate the use of "Uniform Ground Shaking Scenarios" instead of only "Magnitude-Epicentral Location" ones, and other minor improvements were done.

1.2.2. Ground shaking scenarios and damages calculation

Besides a revision of Lisbon Seismic Hazard, here, damages or losses, were derived from the impact of ground shaking in the building stock. As so, the characterization of Lisbon's building stock was a first need.

At the present moment, Lisbon's Building Stock is already organized in 69 different Typologies (49 Masonry Typologies representing about 53% of the whole Building stock and 20 Reinforced Concrete Typologies in representation of the remaining 47% buildings), and for each one of them, Capacity Curves, recently reviewed (Mota de Sá, 2016), have been used with the N2 Method to calculate buildings damages. However, this review required the adaptation of the existing data about buildings distribution along the 3600 urban blocks that exists in Lisbon. This work, was based in Portuguese CENSUS 2011 and, for the special case of Lisbon, the works of C.S Oliveira allowed a crispier differentiation in Lisbon Typologies, especially in what concerns typologies characteristic of the periods from 1755 to 1930, not considered by the CENSUS data.

In what concerns to ground shaking, a "Soils Map" for Lisbon based on previous works of Paula Teves Costa & Isabel Moitinho, later adapted in order to achieve a Soils Classification in accordance with EC8 for the development of previous Seismic Simulators for Lisbon (Mota de Sá, 2009), were used.

1.2.2.1 *Ground Shaking Scenarios*

In order to facilitate Action B.3 where Risk has to be addressed and communicated to non-academic´s audiences, in this task, Risk Scenarios have been developed in two flavors: Uniform Ground Shaking and Magnitude-Epicentral Location. It was a privilege of those involved in Task B.3 to choose the more convenient ones, as also the way of presenting results.

In the domain of Deterministic Scenarios, two processes were be used:

Procedure P1: Uniform Ground shaking (be it measured in Peak Ground Acceleration, PGAS or in Macroseismic Intensities, IEMS).

Procedure P2: Magnitude-Epicentral Location again measured in the same way, but derived from specific scenarios, each one defined by an Epicentral Location and

Magnitude, then translated into PGA's, using some Attenuation Law and Soil Site Amplification.

At the end, a unique scenario is justified and proposed.

Procedure P1: Uniform Ground shaking

Once the aim of this Project resides in the domain of "Non-Structural Losses", even if "Non-Structural Losses" may start to occur at Intensities VI/VII, all possible values of Ground Shaking have been considered once at higher Intensities, more resistant buildings suffered from them. That is, not only Intensities VI or VII should be considered but all the Plausible Range {VI … X} must be taken into account, unless that these higher levels are not plausible in the targeted territory.

So, scenarios for each one of these Intensities (Or PGA's) were simulated.

However, a uniform scenario is not realistic in terms of Intensity, once Site (Soil) effects are present.

Instead, a Uniform Ground Acceleration in Rock Soils, *agr*, could be considered, than, at each site amplified due to Soil Nature that, for the City of Lisbon is illustrated in Figure 2. A possible solution could be to consider several values of *agr* that lead to Intensities {VI, VI, VII, VIII, (IX and X if plausible) in Moderate Soils (Soils from EC8 Class C, with an amplification factor $S_{máx}$=1,6), and then calculate the Macroseismic Intensity in all the city.

To do so, the following expressions were used:

$$IEMS = 7,4 + 3,6.Log_{10}(agr_{m/s^2}) \tag{1}$$

$$\begin{array}{ll} agr < 1\, m/s^2 & : S = S_{\max} \\ 1\, m/s^2 < agr < 4\, m/s^2 & : S = S_{\max} - \dfrac{S_{\max} - 1}{3}(agr - 1) \\ agr \geq 4\, m/s^2 & : S = 1,0 \end{array} \tag{2}$$

Equation (1) was derived using data from several Historical Earthquakes (Both generated Inland and Offshore that targeted Portugal Mainland {1969 M 8,0; 1755 M9,5; 1909 M6,0; 1858, M7.2}. From them, their Magnitude, Epicentral Location and the published Isosseismal Maps were matched using different attenuation Laws considered relevant for

Portugal Mainland (Atkinson & Boore, 2006, 2011; Carvalho, 2009). The cited equation has resulted with a R^2_{adj}=0,98 and is strongly similar with S. Lagomarsino's Law (Lagomarsino, 2006) with a degree of conformity, R^2_{adj}=100%.

Equation (2) is no more than the amplification of the Peak Ground Acceleration, due to Soils effect, suggested in EC8 (CEN, 2010).

By this procedure, the following scenarios were considered as shown in Table 1.

Table 1 – Uniform Scenarios of Ground Shaking to Lisbon. Values for PGA (ag_S, m/s^2) and IEMS in each Soil Class.

Scenario	agr	ag_S (A)	IEMS (A)	ag_S (B)	IEMS (B)	ag_S (C)	IEMS (C)	ag_S (D)	IEMS (D)
1	0.26	0.26	5.3	0.34	5.7	0.41	***6.0***	0.51	6.3
2	0.35	0.35	5.8	0.47	6.2	0.56	***6.5***	0.70	6.8
3	0.48	0.48	6.3	0.65	6.7	0.77	***7.0***	0.97	7.3
4	0.67	0.67	6.8	0.90	7.2	1.07	***7.5***	1.33	7.8
5	0.92	0.92	7.3	1.24	7.7	1.47	***8.0***	1.83	8.3
6	1.31	1.31	7.8	1.73	8.3	2.02	***8.5***	2.49	8.8
7	1.98	1.98	8.5	2.45	8.8	2.78	***9.0***	3.32	9.3

These scenarios are here presented in Figure 2 to 9.

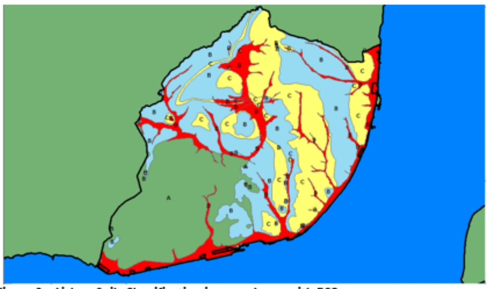

Figure 2 – Lisbon Soils Classification in accordance with EC8.

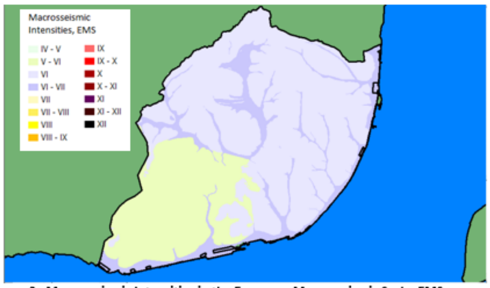

Figure 3– Macrosseismic Intensities in the European Macrosseismic Scale, EMS, generated by a uniform Peak Ground Acceleration in Rock Soils, agr=0,26 m/s².

Figure 4 – Macrosseismic Intensities in the European Macrosseismic Scale, EMS, generated by a uniform Peak Ground Acceleration in Rock Soils, agr=0,35 m/s².

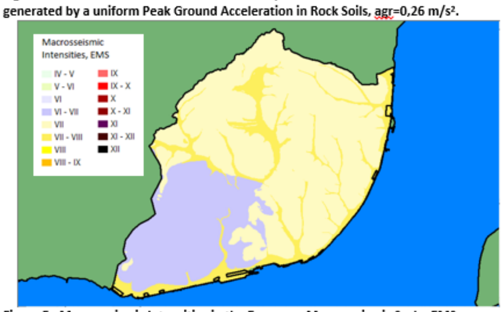

Figure 5– Macrosseismic Intensities in the European Macrosseismic Scale, EMS, generated by a uniform Peak Ground Acceleration in Rock Soils, agr=0,48 m/s².

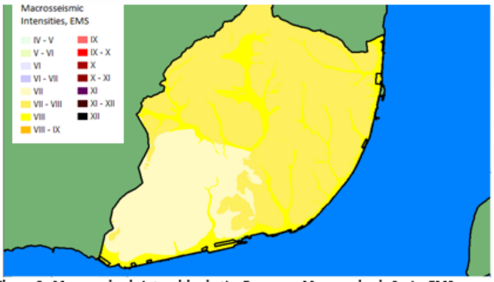

Figure 6– Macrosseismic Intensities in the European Macrosseismic Scale, EMS, generated by a uniform Peak Ground Acceleration in Rock Soils, agr=0,67 m/s².

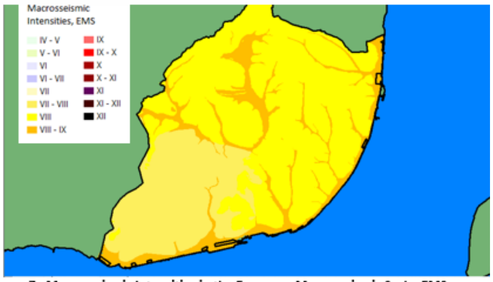

Figure 7– Macrosseismic Intensities in the European Macrosseismic Scale, EMS, generated by a uniform Peak Ground Acceleration in Rock Soils, agr=0,91 m/s².

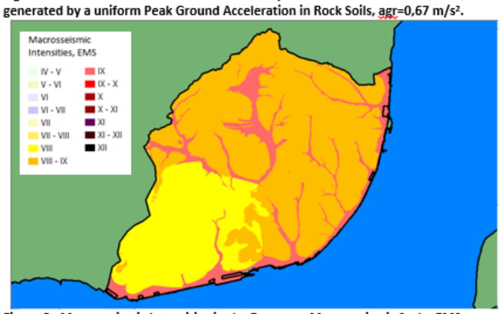

Figure 8– Macrosseismic Intensities in the European Macrosseismic Scale, EMS, generated by a uniform Peak Ground Acceleration in Rock Soils, agr=1,31 m/s².

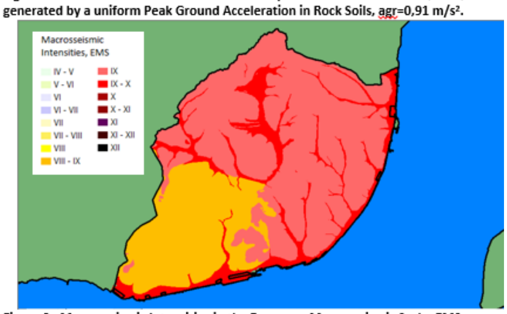

Figure 9– Macrosseismic Intensities in the European Macrosseismic Scale, EMS, generated by a uniform Peak Ground Acceleration in Rock Soils, agr=1,98 m/s².

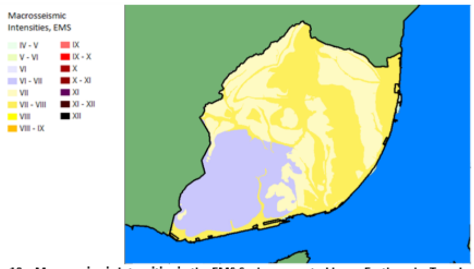

Figure 10 – Macrosseismic Intensities in the EMS Scale, generated by an Earthquake Type I, with Peak Ground Accelerations in Rock of 0,51 m/s², with a Return Period of 95 Years.

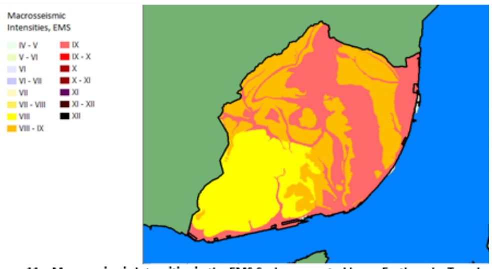

Figure 11 – Macrosseismic Intensities in the EMS Scale, generated by an Earthquake Type I, with Peak Ground Accelerations in Rock of 1,5 m/s², with a Return Period of 475 Years.

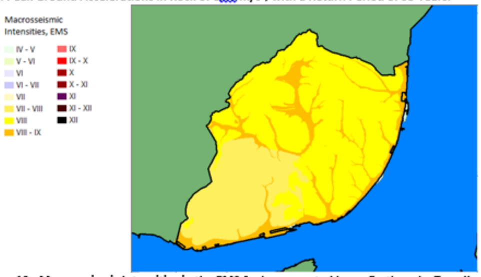

Figure 12 - Macrosseismic Intensities in the EMS Scale, generated by an Earthquake Type II, with Peak Ground Accelerations in Rock of 0,89 m/s², with a Return Period of 95 Years.

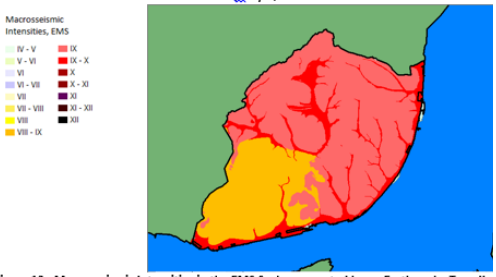

Figure 13 - Macrosseismic Intensities in the EMS Scale, generated by an Earthquake Type II, with Peak Ground Accelerations in Rock of 1,7 m/s², with a Return Period of 475 Years.

Beside the above scenarios, others are also of interest.

With Risk defined as the likelihood of failing some target, then, one can elect as targets, or as objectives, the ones prescribed in Eurocode:

- The "Damages Limitation", by which Functional/Non-Structural Damages should be avoided, not occurring with a probability higher than 10% in 10 years (corresponding to a Return Period, TR 95 years), and
- The "Collapse Limitation", by which Collapses occurrence should not exceed a probability of 10% in 50 Years (TR 475 Years).

Once, in Portugal, two Earthquake Types can be responsible for these scenarios, one defined 4 cases of Uniform Ground Shaking in terms of uniform accelerations agr_j (m/s^2)*, as shown in*

Table 2, where agr_j was obtained by Eq (3).

$$agr_j = agr_i \left(\frac{TR_j}{TR_i} \right)^{1/k} \tag{3}$$

Table 2 – Scenarios of Uniform ground accelerations, agr_j (m/s²)

	Years	*Years*	*m/s²*		*m/s²*	
EQ Type	**TR_i**	**TR_j**	**agr_i**	**k**	**agr_j**	**Objective**
I	475	95	1.50	1.5	0.51	Non-Damages Limitation
I	475	475	1.50	1.5	1.50	Collapses Limitation
II	475	95	1.70	2.5	0.89	Non-Damages Limitation
II	475	475	1.70	2.5	1.70	Collapses Limitation

The above scenarios are illustrated in Figures 10 to 13, and their expective damages are reported in Table 3. From tat, some consideratios seem of interest.

From the same Table (Table 3), one can observe from the figures in row 3 and 4th, that regardless of an higher acceleration of 1,70 m/s² generated by an earthquaque type II, damages from this scenario are much lower than the ones genereted by the scenario in row 4, with a lower acceleration of 1,50 m/s² generated by an earthquaque type I. This illustrates the influence of spectral frequency contents, with a corner period TC=0,25 s in the first case and TC=0,6 s in the second one. In fact, and in the Lisbon case, where higly fragile (low ductility) and rigid (high frequency) massonry structures represents more than 50% of the whole building stock, are expected to suffer very high damages when targeted by an earthquake Type I, being responsible by higher damages in this cases. This was one of the the reasons by which, in this studdy, damages expectations were calculated by the N2 method, instead of using a Macroseismic one, this last one based in Macroseismic Intensity and blind in what concerns the frequency contents of the Demand Spectra that in Portugal assumes two different shapes according to the type of eartquake (seismogenic source) being considered.

In fact, one can easily be induced in error while observing Figures 2 to 13, where Intensity Maps for several levels of PGA (Peak Ground Acceleration) are shown.

So, as a 1st conclusion, one can state that "Intensity Maps" generated as above constitute a biased representation of Seismic Risk and, by so, should not be considered to communcation purposes.

Table 3 – Expected damages from EC8, Portuguese Annex, and some Historical Earthquakes (PGAs – Peak Ground acceleration at surface)

					Damages Expectations				
	Years	*m/s²*	Earthquake	Mean Damage	None	Sligth	Moderate	Extensive	Global
P[ ]	**TR**	**agr**	**Type**	**Grade {0…4}**	**% Dg 0**	**% Dg 1**	**% Dg 2**	**% Dg 3**	**% Dg 4**
10% / 10 years	95	0.89	II	1.4	36%	21%	25%	15%	7%
10% / 10 years	95	0.51	I	1.2	44%	21%	16%	12%	7%
10% / 50 years	475	1.70	II	2.1	8%	21%	32%	29%	9%
10% / 50 years	475	1.50	I	3.1	9%	9%	8%	23%	54%
Year 1551, Mw 7.1, 28 km, *PGAs (m/s²){1,56…3,62}*			II	2.3	21%	8%	17%	27%	27%
Year 1755, Mw 8,7, 227 km, *PGAs (m/s²){0,86…2,10}*			I	2.5	15%	11%	15%	26%	33%
Year 1926, Mw 5,5, 7 km, *PGAs (m/s²){0,44…1,99}*			II	0.6	67%	16%	10%	5%	2%
Year 1969, Mw 8,0, 320 km, *PGAs (m/s²){0,27…0,59}*			I	0.3	82%	11%	4%	2%	1%

Table 4), *Expectations and consequences for some Catalogue Scenarios meaningful to Lisbon are shown.*

There, the following values are shown:

Year Earthquake Year,
Type Earthquake Type,
Median agr Median Peak Ground Acceleration in Rock (from *QuakeIST),*
TR Return Period of *agr* in accordance to Eq (4),
P[x≥1|Δt=50 years] *Exceedance probability of* agr *during an Exposure Period of 50 years, in accordance to Eq (4). Values of* agr_i *and* k *as shown in*

Table 2,
Sligth-Moderate Percentage of Buildings with Damage Grades {1; 2},
Extensive-Global Percentage of Buildings with Damage Grades {3; 4}.

$$TR_j = 475.\left(\frac{agr_j}{agr_i}\right)^k \tag{4}$$

$$P[x \geq 1 \mid \Delta t] = 1 - e^{-\frac{\Delta t}{TR}} \tag{5}$$

Table 4 – Expectations for an Exposure Period of 50 Years, taken from scenarios registered in the Portuguese Seismic Catalog (meaningful to Lisbon).

Year	Type	Median agr(m/s^2)	TR	P[x≥1|50 years]	Slight- -Moderate	Extensive- -Global
1551	II	1.84	579	8%	15%	54%
1755	I	1.00	259	18%	26%	59%
1926	II	0.51	23	88%	26%	7%
1969	I	0.28	38	73%	15%	3%

At a first glance, one could conclude from this Table 4, that it seems clear that Scenarios with the highest probability of occurrence are of most importance to the prevention of Non-Structural Damages. Be it because of their high probability, but also because scenarios with larger Return Period leads to such high Structural Damages that prevention of Non-Structural ones becomes less important.

But, a closer look to expectations from a less probable scenario (TR 475 years, P[Exceedance | 50 years] = 10%, due to Earthquakes Type II can generate significant Non-Structural Damages both in Masonry and in RC buildings as shown in *Table 5*.

Here, one can observe that in Masonry structures Moderate-Extensive Damages represent ~ 67% while Extensive-Total are of about 44%. This difference is even more important in RC buildings where Moderate-Extensive damages are ~ 45% while Extensive-Total are of about 24%.

Table 5 – Damages expectations in masonry and RC buildings, due to an Uniform acceleration in Rock, PGA = 1,70 m/s², TR 475 years, P[Exceedance] 10% / 50 years, due to an Earthquake Type II. (Values Simulated by QuakeIST).

Massonry	N	No Damges	Light	Moder.	Extens.	Global
	29854	1375	5548	10219	9934	2777
%[Dg=k]		5%	19%	34%	33%	9%
P[Dg≥k]		100%	95%	77%	43%	9%

RC	N	No Damges	Light	Moder.	Extens.	Global
	10446	1973	3082	2869	1860	662
%[Dg=k]		19%	30%	27%	18%	6%
P[Dg≥k]		100%	81%	52%	24%	6%

From the above considerations, it seems reasonable to purpose that in order to address the prevention of Non-Structural Damages following possible Earthquakes, in Lisbon:

- The low Probability Scenario generated by Earthquakes Type I with a Return Period of 475 years, seams of no much interest, not only due to low probabilities, but especially because of its high percentage of High-Level Damages (54% from the 1551 Scenario and 59% from the 1755 one, against 15% and 26% lower damages in these scenarios, respectively).
- However, the first 3 scenarios shown in Table 3 are of concern. The first two are more probable (TR 95 Years, P[Exceedance]=10% / 10 years, while the 3rd one, with a Return Period of 475 years, even with a lower probability is also of high concern.

This is recapped here in Table 6.

Table 6 – Retrieved scenarios as meaningful for Non-Structural Damages Prevention.

				Damages Expectations				
	Years	Earthquake	Mean Damage	None	Sligth	Moderate	Extensive	Global
P[ ]	TR	Type	Grade {0…4}	% Dg 0	% Dg 1	% Dg 2	% Dg 3	% Dg 4
10% / 10 years	95	II	1.4	36%	21%	25%	15%	7%
10% / 10 years	95	I	1.2	44%	21%	16%	12%	7%
10% / 50 years	475	II	2.1	8%	21%	32%	29%	9%

Here arrived, the choice of a unique Reference Scenario has to be made. But, before to do so, it may be also of interest to look at some of the historical earthquakes that targeted the city of Lisbon.

Procedure P2: Magnitude-Epicentral Location

In this procedure, several scenarios were generated based in Real Earthquakes that targeted Portugal Mainland. These episodes were selected by the fact that they were simply felt or caused minor damages, while others caused severe human injuries and damages in the Portuguese building stock. In Figure 14 and in Figure 15 their epicentral location and year are shown.

Figure 14 – Epicenter Location for Inshore (Near) Earthquakes that affected Lisbon (in the last 1000 years).

Figure 15 - Epicenter Location Offshore (Far) Earthquakes that affected Lisbon (in the last 1000 years). (The 2009 earthquake was mainly felt in the Southern Region of the Country, Algarve (Faro), and only slightly felt (Intensity III-IV) in Lisbon.

Their impact, translated by Intensities Maps are shown in Figure 16, Figure 17, Figure 18, Figure 19, Figure 20, Figure 21, Figure 22, Figure 23, Figure 24, Figure 25, Figure 26 and Figure 27.

By the reasons above said, and in accordance with Table 6, there are 3 scenarios that may be candidates to be used in this study. Furthermore, from pure probabilities, Earthquakes with a Return Period of 95 years are more probable to occur. But in what concerns to the

Earthquake Type to be used (I or II), it can be seen in Figure 14 and Figure 15, that there are more Near Source Earthquakes than Far sources affecting Lisbon. As a simple, but also arguable rule, one is more willing to select a Near Source Earthquake than a Far Source one. This choice could also be sustained by the fact that in the Seismic Catalog, the number of earthquakes that reached Lisbon with Intensities ≥ VI, is not significantly different between the two types of Earthquakes.

By this rule, and coming back to Table 6, the Far-Source (Type I) earthquake there shown in row 2, may be discarded. This can also be supported by the fact that the 1st scenario with equal probability (shown in the first row of that table) is more interesting for the purposes of this work with 65% of Light-Extensive damages while the Type I has 49% of such damages.

Being so, at this point, the choice can go to a Type II (Near Source) scenario but with different Return Periods (95 or 475 years).

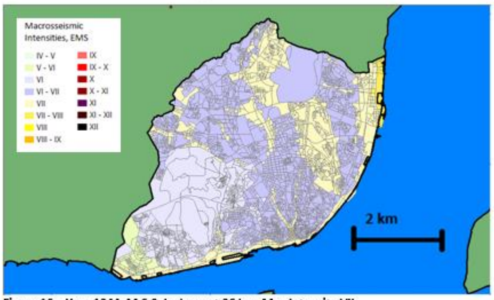

Figure 16 – Year 1344, M 6,0, Inshore at 36 km. Max Intensity VII.

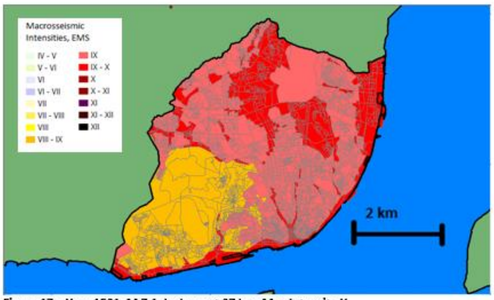

Figure 17 – Year 1531, M 7,1, Inshore at 27 km. Max Intensity X.

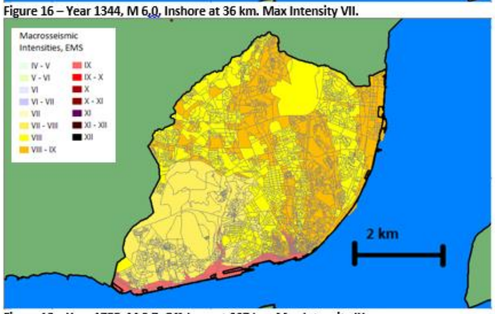

Figure 18 – Year 1755, M 8,7, Offshore at 227 km. Max Intensity IX.

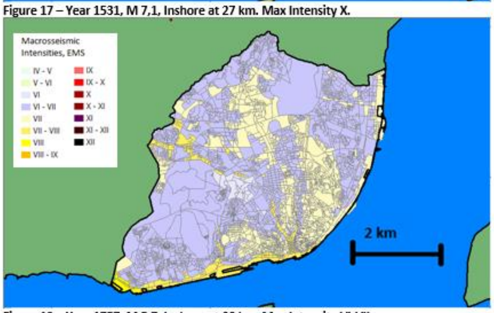

Figure 19 – Year 1757, M 5,7, Inshore at 20 km. Max Intensity VI-VII.

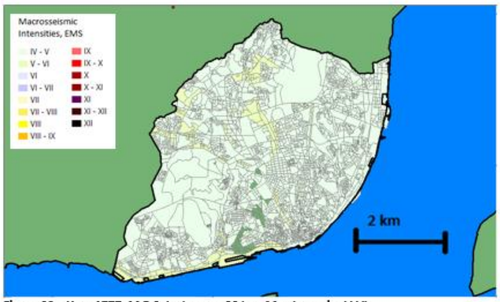

Figure 20 – Year 1777, M 5,0, Inshore at 30 km. Max Intensity V-VI.

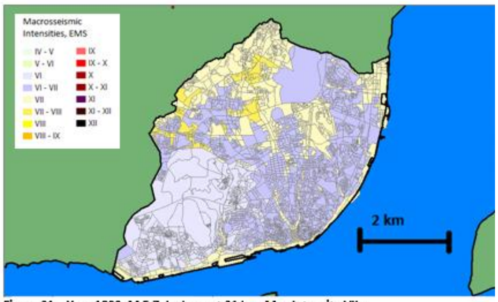

Figure 21 – Year 1899, M 5,7, Inshore at 21 km. Max Intensity VII.

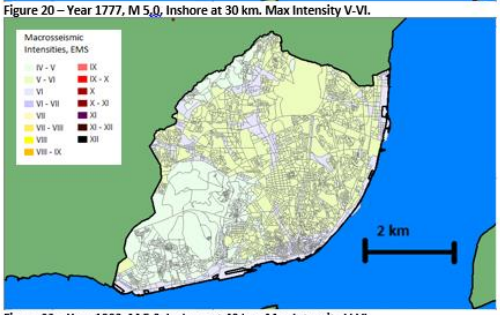

Figure 22 – Year 1903, M 5,0, Inshore at 40 km. Max Intensity V-VI.

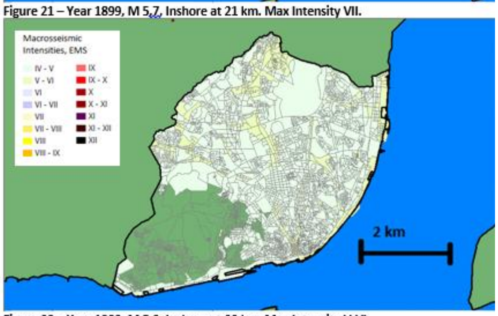

Figure 23 – Year 1909, M 5,0, Inshore at 29 km. Max Intensity V-VI.

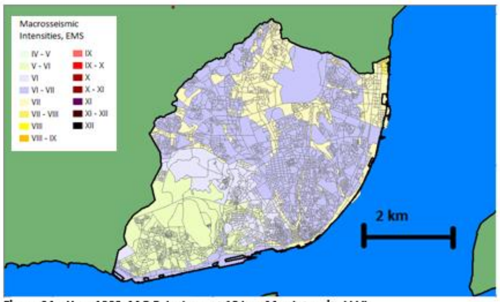

Figure 24 – Year 1909, M 5,5, Inshore at 18 km. Max Intensity V-VI.

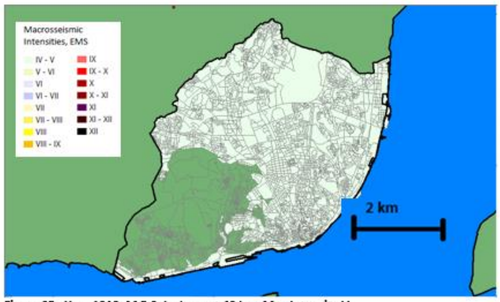

Figure 25– Year 1913, M 5,0, Inshore at 40 km. Max Intensity V.

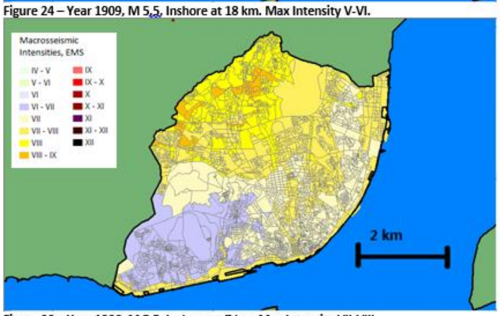

Figure 26 – Year 1926, M 5,5, Inshore at 7 km. Max Intensity VII-VIII.

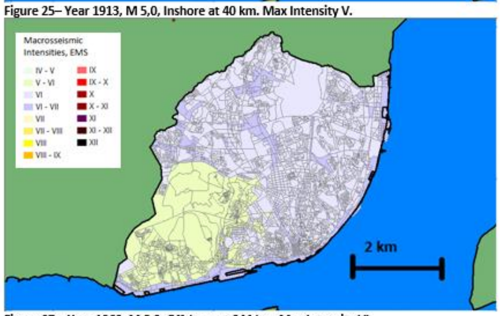

Figure 27 – Year 1969, M 8,0, Offshore at 344 km. Max Intensity VI.

Two rules can be used to choose among them:

- Choose the more Probable,
- Choose the more Destructive. Not so probable BUT EQUALLY PLAUSIBLE.

Reasons in favor and against each one of them exists and are not consensual among the scientific community. So, which one to choose? It is one's opinion that, once Global Damages are almost equal in both scenarios, the stronger one should be chosen. But, if this reasoning is not enough to choose the more severe (but equally plausible) one, after visiting the recent occurrences in Italy (L'Aquila, Amatrice and Norcia), it becomes clear that if citizens from Norcia had pursued the "Probabilistic" and not the "Plausible" scenario, they would be, today, in the same situation that citizens from the other Villages/Cities.

From that, it seems that a Type II scenario with Return Period of 475 years, may be the most adequate in order to communicate and too be used in this work.

Now, one has to decide between an "EC8 Uniform Scenario" or between a fictitious one.From that, it can be argued that due to the nature of Near-Sources, these events have a rapid attenuation, and taking into account that Lisbon has about 80 km2 Area, a path across the city can reach distances of about 15km, along which accelerations may have a not insignificant difference. This is even more influential if one take into consideration the opinion expressed by Vilanova & Fonseca (Vilanova & Fonseca, 2004) by which, a Magnitude 6,5-7,0 with a Return Period of 200 years can be expected from the Lower Tagus Valley Fault and also the location of historical earthquakes around Lisbon as mapped in Figure 28.

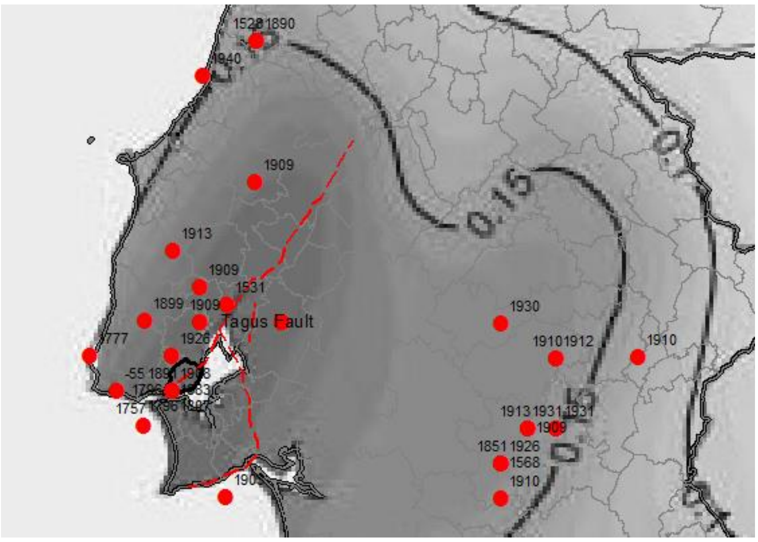

Figure 28 – Low Tagus River Fault (Red dashed line), Historic Earthquakes and Hazard Map proposed by Vilanova & Fonseca for Earthquakes Type II, Lisbon.

If that is so (agr ~ 1,6 … 2,0 m/s^2 / TR 475 Years), then by Eq (3), in an Exposure Period of 95 years, accelerations can reach the value of[a] 1,1 m/s^2. Now, taking into consideration the Alexandra Carvalho Attenuation Law for Earthquakes Type II (Carvalho, 2008), such a scenario can be simulated by a M 6,5 located at about 15 km NE of Lisbon, as indicated in Figure 30 by which these accelerations can be achieved (Figure 29). This can then become a Reference Scenario as illustrated in Figure 31.

[a] $1,1 \sim 2,0.(95/475)^{1/2.5}$

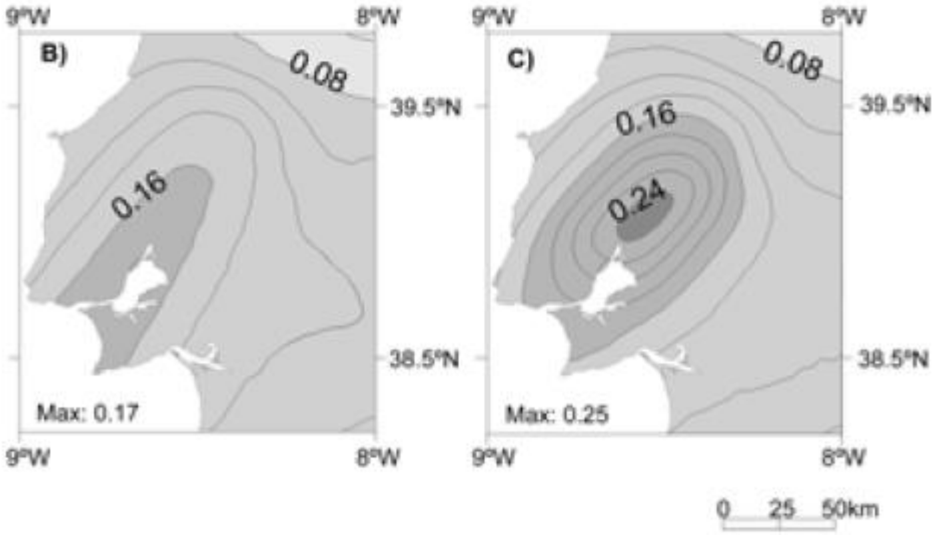

Figure 29 – Seismic Hazard in Lisbon from Near Sources of the Low Tagus River Faults (Earthquakes Type II) for a Return Period of 475 years (Exceedance Probability 10% / 50 years) in accordance with Vilanova & Fonseca. The two Figures correspond to different plausible rupture scenarios.

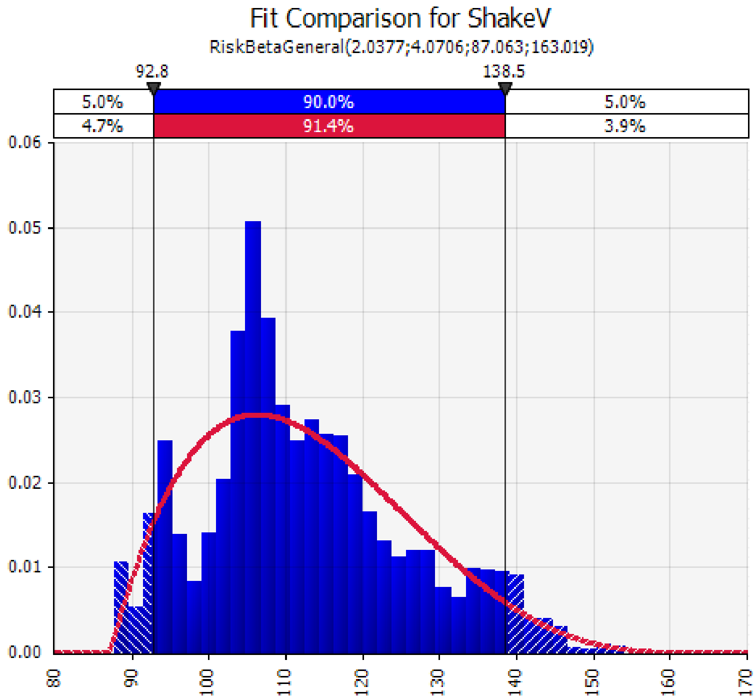

Figure 30 – PGAr (cm/s2), along Lisbon, from M 6,5 ~ 15km NE Lisbon (Mode: 1,1 m/s2, Median: 1,10 m/s2 Mean 1,12 m/s2). Surface PGA and Macroseismic Intensities are mapped in Figure 34 and in Figure 35 respectively.

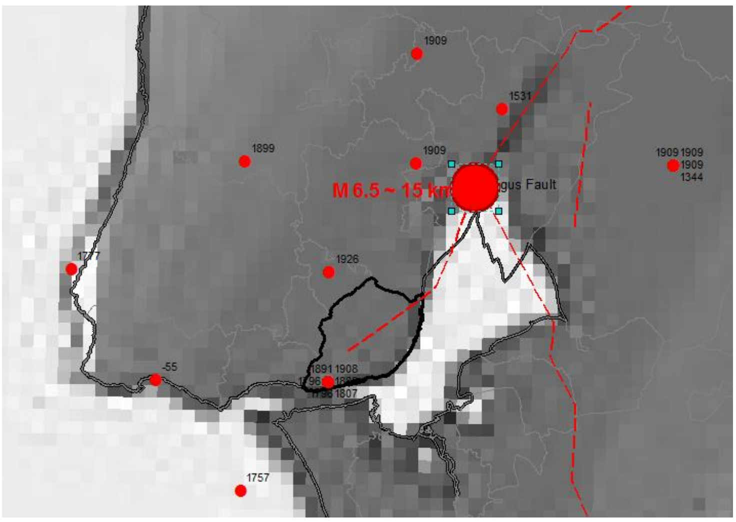

Figure 31 – Magnitude 6,5 and Epicentral location for the Reference scenario.

Table 7 – Expected Damages from the Reference scenario (TR 95 years).

Epicenter Located in the Low Tagus River Fault, at about 15 km from Lisbon, with an Average, PGAr = 1,12 m/s^2.

Intensities (EMSS) {7,2 ...9,0} *Surface PGA (m/s^2) {0,89 ...2,80}*

Total	N	%	No Damges	Light	Moder.	Extens.	Global
Massonry	27144	57%	166	1321	4475	9084	12097
RC	20668	43%	6926	4118	2933	3221	3470
	47812		7091	5439	7409	12305	15568
%[Dg=k]			15%	11%	15%	26%	33%
P[Dg>k]				85%	74%	58%	33%

Massonry	N	No Damges	Light	Moder.	Extens.	Global
	27144	166	1321	4475	9084	12097
%[Dg=k]		1%	5%	16%	33%	45%
P[Dg≥k]		100%	99%	95%	78%	45%

RC	N	No Damges	Light	Moder.	Extens.	Global
	20668	6926	4118	2933	3221	3470
%[Dg=k]		34%	20%	14%	16%	17%
P[Dg≥k]		100%	66%	47%	32%	17%

From the above figure, one can then say that:

1. The EC8 Objective of "Damages Limitation" (Non-Structural Losses) is violated in 58 % - 74% of all buildings (Damage Grades 2- Moderate Damages to Extensive Damages- Damage Grade 3).

2. This figures correspond to a violation of the objective in 78%-95% in Masonry buildings (that, in accordance to CENSUS 2011(INE, 2011) represent about 57% of the whole building stock) and in 32%-47% of Reinforced Concrete buildings (representative, in accordance with the same source, of about 43% of the whole building stock).

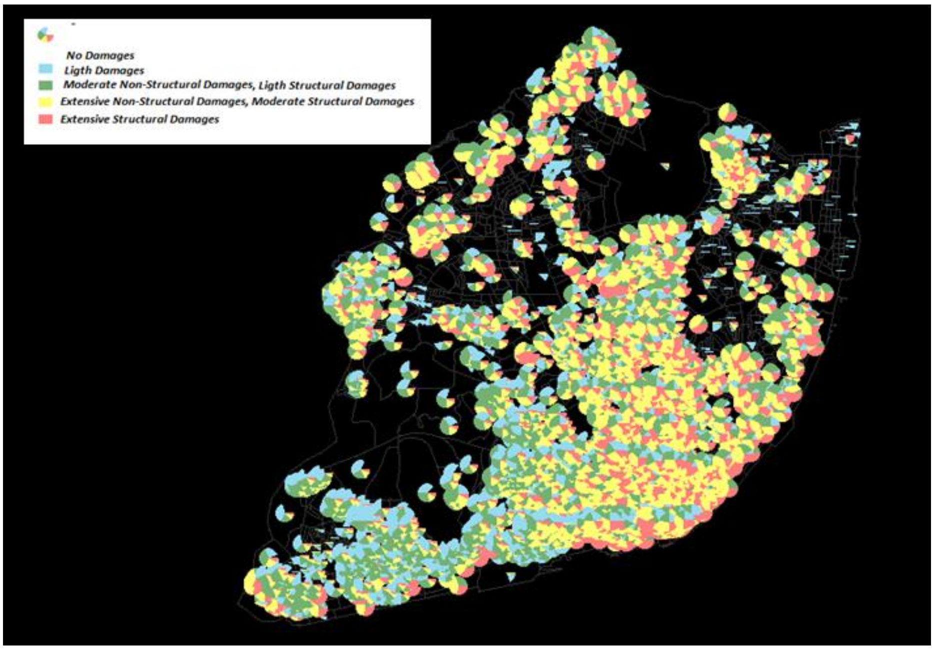

Figure 32 – Pictorial representation of the Reference Scenario.

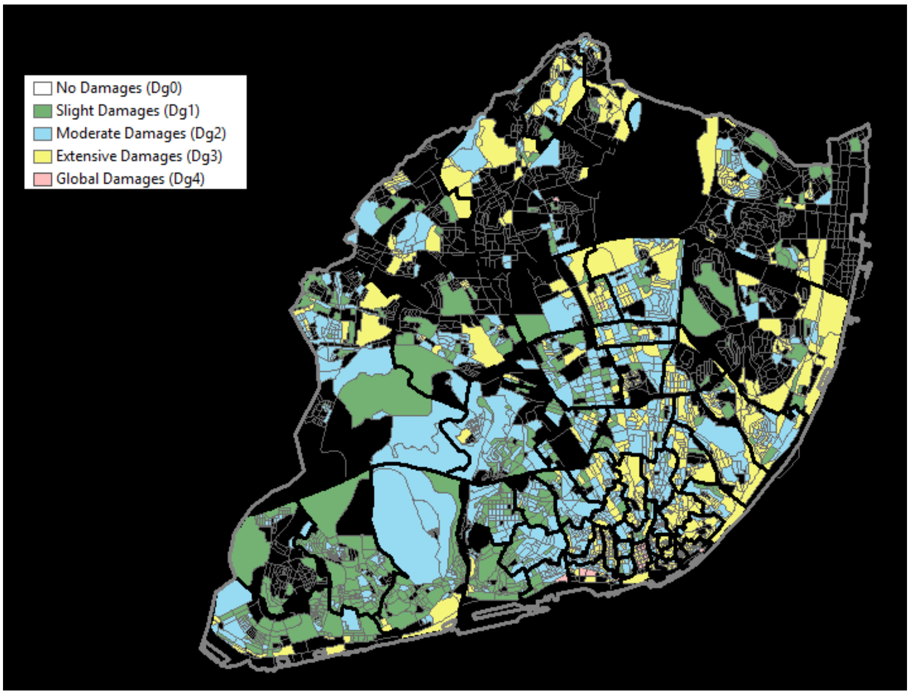

Figure 33 – Alternative representation of expected damages from the Reference Scenario, here using "Averaged" values of "Mean Damage Grades".

Figure 34- Expected Surface PGA (m/s2) from the Reference scenario.

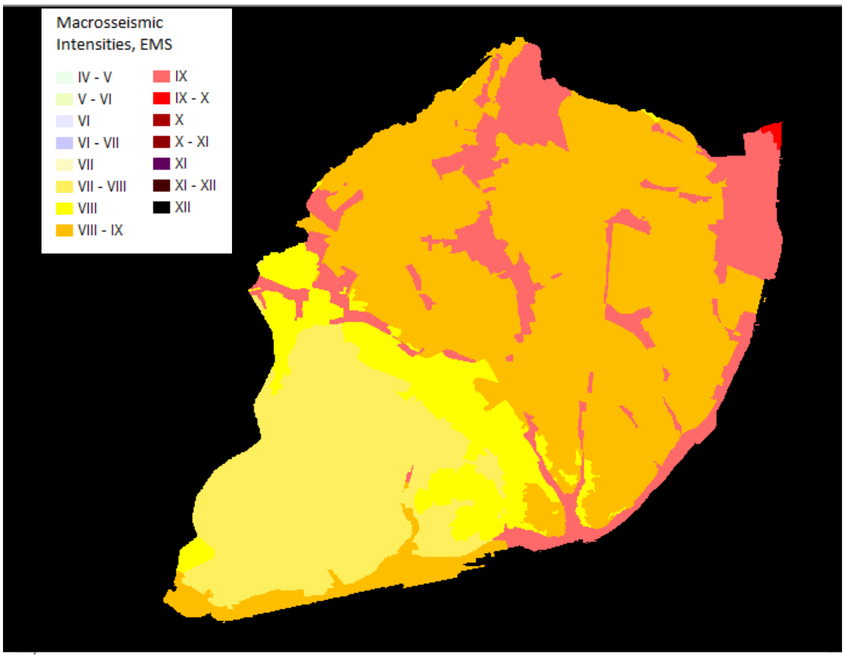

Figure 35 - Expected Macroseismic Intensities from the Reference scenario.

1.3 SEISMIC SCENARIOS FOR MT. ETNA PILOT AREA

1.3.1. Introduction

Simulating the effects produced by an earthquake is a multidisciplinary field of investigation aimed at assessing the level of seismic risk to which an area is exposed. A variety of methods, leading to deterministic or probabilistic seismic scenarios, have been developed according to different levels of accuracy required - the most complete generally being based on numerical models that take account of ground-motion predictive relationships (expressed in acceleration, velocity or displacement), local geologic conditions (site effects), historical macroseismic intensity data, together with building typologies and their vulnerability. These seismic scenarios are normally envisaged for large cities and refer to the strongest earthquakes or their occurrence probability.

On the other hand, a simplified approach, adopted worldwide, that provides a preliminary, semi-quantitative assessment of the level of shaking and extent of potential earthquake hazard, is obtained through the software package ShakeMap (Wald et al., 1999). This procedure seeks to automatically estimate, in a few minutes, the level of expected ground shaking using real-time data acquired by a seismic network, which are converted into maps of peak ground acceleration (PGA), peak ground velocity (PGV) and macroseismic intensity.

However, ShakeMap as it stands cannot be used at Etna region due to the different attenuation and scaling laws of purely tectonic earthquakes vs volcano-tectonic events (Rovelli et al., 1988; McNutt, 2005; Giampiccolo et al., 2007).

The problem of seismic scenarios at Mt. Etna has been tackled in terms of macroseismic intensity, adopting the probabilistic approach based on the Bayesian statistics (Rotondi and Zonno, 2004) proposed by Azzaro et al. (2013).

According to two attenuation models, isotropic (point source, symmetric decay) and anisotropic (linear source, decay depending on the direction), the method calculates the probabilistic distribution of the intensity at a given site (I_S) conditioned on the epicentral intensity (I_0) of the earthquake and the epicentre-site distance through a binomial-beta model (Zonno et al., 2009).

A detailed analysis of occurrence probability of shaking is the first step in the process of seismic risk evaluation since it provides indications for eventual interventions and allows the definition of possible earthquake scenarios. In particular, the disaggregated data analysis performed on some key localities of the study area, enabled defining the "design earthquake" - and hence the causative fault - which most contributes to the seismic hazard at a site-scale.

1.3.2. Seismic hazard

Earthquakes are by far the most important source of hazard for the densely urbanized areas of Mt. Etna. Despite its low energy ($M_W \leq 5.3$), volcano-tectonic seismicity is capable of producing severe damage and even destruction, due to the shallow nature of hypocenters (Azzaro, 2004; Alparone et al., 2015). Macroseismic intensity at the epicentre may even reach degree IX on the EMS (European Macroseismic Scale, see Grünthal, 1998) but fortunately the related strong ground motions affect small areas owing to the rapid attenuation of seismic intensity that is typical of volcanic regions (Azzaro et al. 2006; Azzaro et al., 2013b and references therein). Studies aimed at assessing seismic hazard at Mt. Etna have been undertaken in the last years by means of a probabilistic approach based on the use of macroseismic data - "site approach" (Albarello and Mucciarelli 2002) - whose computational procedure was implemented by D'Amico and Albarello (2008) in the SASHA code.

The contribution of the volcano-tectonic sources to the seismic hazard at a local scale was investigated by Azzaro et al. (2008, 2013a), exploiting the huge historical dataset of earthquakes available for this area. In brief, these analyses have demonstrated that seismic hazard in the Etna region is determined by two distinct seismotectonic regimes, namely regional earthquakes occurring in eastern Sicily ($6.2 \leq M_W \leq 7.4$) and local events due to seismic sources in the area of the volcano, each characterized by different magnitude ranges and occurrence rates. The former prevail on long exposure times (50 years), the latter on shorter exposure times (30 years or less), producing the same values of intensity (VIII and IX degree) in the sites located along some of the main seismogenic faults affecting the eastern flank of Etna.

In the framework of the aims of the project, the Probabilistic Seismic Hazard Assessment (PSHA) was computed by considering a time series of macroseismic intensities at the site of interest (i.e. the local seismic history). These time series were compiled by combining seismic effects observed at the site during past earthquakes, and, when needed, 'virtual' intensities deduced from epicentral data through an attenuation relationship. Each intensity evaluation was considered as being affected by a measurable uncertainty, which depends on the available information. Completeness of the information that was locally available, was then evaluated along with the relevant uncertainty (local completeness). The seismic recurrence at the site was parameterised for each intensity threshold I, using a fully distribution-free approach that does not require any pre-processing (e.g. aftershock removal, selection of mainshocks within a seismic sequence).

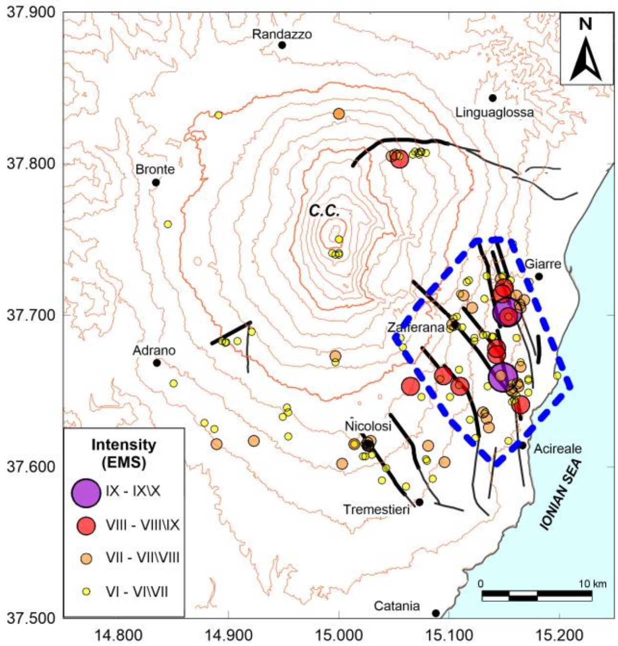

Figure 36. Map of damaging earthquakes ($I_0 \geq$ VI EMS) occurring in the Etna area from 1600 to 2013 (data from CMTE Working Group, 2014; Azzaro and Castelli, 2015). Solid black lines indicat e the main active faults (from Azzaro et al., 2012); blue dashed lines show the studied area and the Timpe Fault System; C.C. central craters of Etna.

The SASHA code was used that provides i) hazard curves (i.e. probability that at least one event with intensity not less than I_S will occur in the exposure time at the site under study); ii) reference intensity I_{REF} (which is determined from the hazard curve as a function of the probability threshold considered); iii) magnitude/distance pairs that are more representative for the reference ground motion (disaggregation).

The intensity database and earthquake parameters of the Macroseismic Catalogue of Etnean Earthquakes (CMTE Working Group, 2014), which lists earthquakes in the Mt. Etna area from 1832 to 2013, was used as input data. This dataset was extended as far back as the year 1600, with new data coming from recent historical investigations (Azzaro and Castelli, 2015). For the aims of the present work, only the earthquakes above the damage threshold (epicentral intensity $I_0 \geq$ VI EMS) were considered, obtaining a dataset of 4,432 intensity values referring to 140 events, with moment magnitudes ranging from 3.7 to 5.3. As shown in Figure 36, most seismicity is located in Etna's eastern flank, though it is noteworthy that all the destructive events (some ten with $I_0 \geq$ VIII EMS) occur in the area among the towns of Acireale, Giarre and Zafferana, the most populated sector of the volcano (Meroni et al., 2016). These earthquakes are due to the seismotectonic activity of the Timpe fault system (Azzaro et al., 2012).

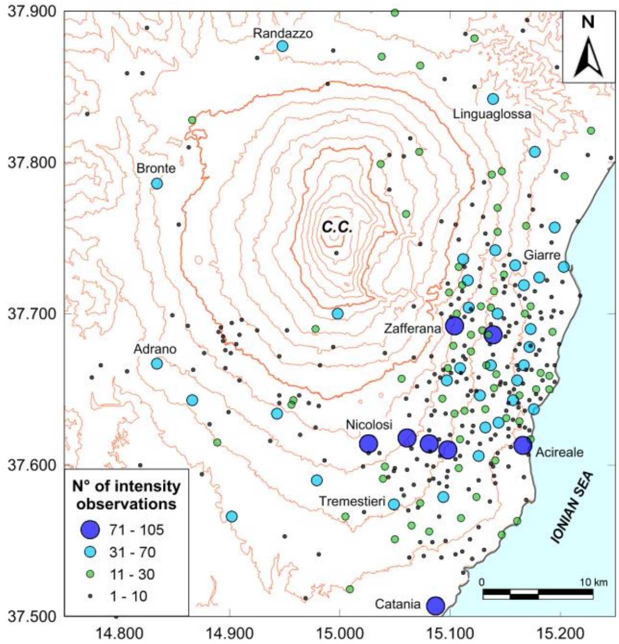

Figure 37. Distribution and number of intensity observations for the localities reported in the macroseismic database, referred to the earthquakes above the damage threshold ($I_0 \geq$ VI EMS) considered in the study.

Regarding the distribution of the observed intensity data related to these events, Figure 37 shows that the 415 localities (53 of which are municipalities) reported in the macroseismic database are "clustered" in the eastern flank, where there are major settlements - the city of Catania included - characterized by exceptionally well documented seismic histories (71-105 intensity data per site). Among them, the towns of Acireale and Zafferana, located on the boundary of the Timpe seismogenic zone (see Figure), have more than 100 observations each.

To improve the completeness of the site seismic histories, the dataset of the observed intensities has been integrated with "virtual" values calculated through a probabilistic attenuation model, starting from the epicentral parameters (coordinates, I_0) of the earthquakes reported in the CMTE catalogue. This solution was applied only if the intensity data related to a given earthquake in the considered locality was missing. For the probabilistic attenuation model, the one calculated in the framework of the UPStrat-MAFA project (Sigbjörnsson et al., 2016) by Rotondi et al. (2016) was used. Although the localities whose seismic history is well documented represent about 30% (112) of the sites considered in the hazard analysis, most of them appear densely distributed on the sector of the volcano most exposed to earthquake impact. This ensures that the contribution of real data (i.e. macroseismic intensities) in reconstructing the integrated seismic histories (observed plus calculated data) of important localities is prevalent.

1.3.3. Occurrence probability of non-structural damage

As described in the EMS scale (Grünthal, 1998), the non-structural damage (grade 1, 2 and 3) may be confined mainly between the VI and the VII degrees, while starting from VIII the contribution of structural damage becomes more relevant (grade 3, 4 and 5). For this reason the seismic hazard has been mapped (Figure 38) as occurrence probability for the selected expected intensity (I_{EXP}), rather than in the more common form of I_{EXP} for the exceeding probability.

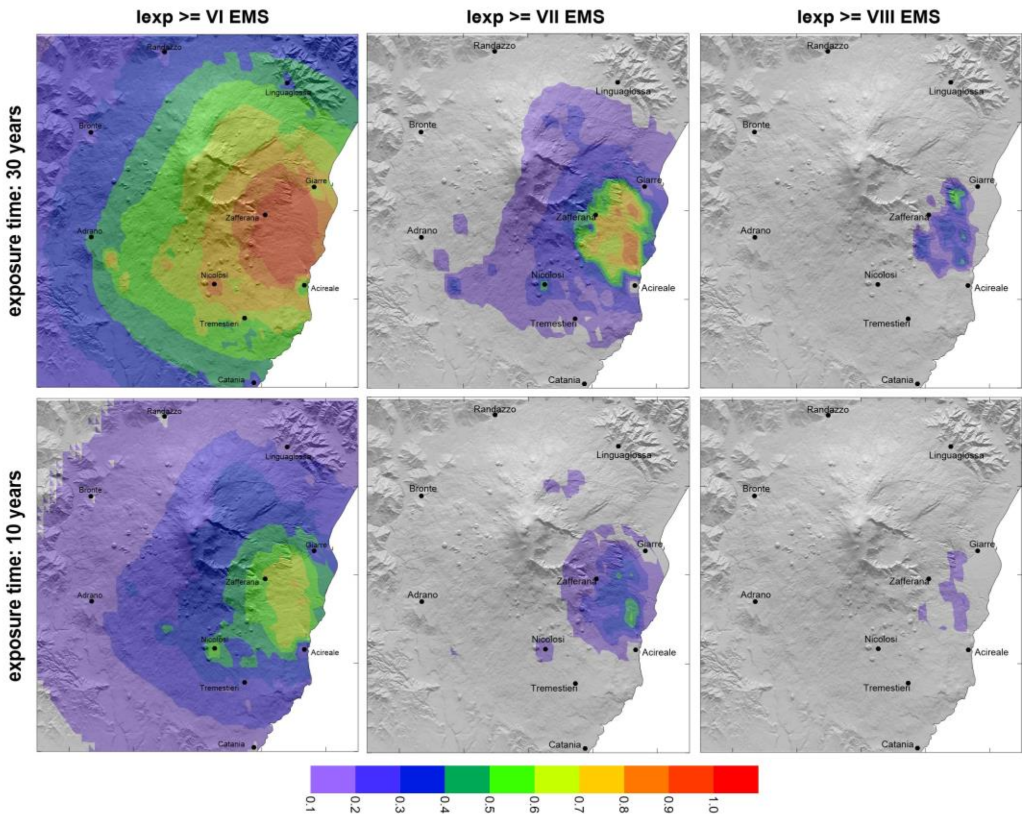

Figure 38. Maps of the occurrence probability for expected intensity I_{exp} calculated for the exposure times of 30 and 10 years.

Figure 38 shows that settlements located in the eastern flank of Mt. Etna have a high probability (> 80% in 30 years; > 50% in 10 years) of undergoing shaking capable of producing slight non-structural damage (at least VI EMS). The probability of large non-structural damage (at least VII EMS) is greater than 50% for 30 years of exposure time for the entire eastern flank, and is greater than 10% in 10 years. This analysis confirms the high seismic hazard of this sector of the volcano, not only for destructive events but also for moderate energy earthquakes.

The village of Zafferana Etnea has a probability greater than 50% to be struck with an intensity at least of VII EMS in 30 years. This result is in agreement with the maximum observed intensity (I_{MAX} = VII EMS) for this locality, reported in 1984 (CMTE Working Group, 2014), and allows selecting this village as a reliable site for the disaggregation analysis.

1.3.4. Disaggregation analysis

A disaggregation analysis was performed to determine the most representative earthquakes that contribute to the hazard for the test site of Zafferana Etnea, located in the eastern flank of Mt. Etna.

The starting point was the value of I_{REF} obtained by the statistical analysis of the seismic history. On this basis, a search of the past earthquakes that contributed most to the hazard was carried out. Since the events are characterized in terms of magnitude and epicentral location, it is possible to identify the most significant magnitude/distance bins, namely the "design earthquake". In this framework, the "design earthquake" represents a class of seismic events that actually occurred in the past and that can be identified. It is worth noting that it does not necessarily correspond to a single earthquake, since a number of events located at similar epicentral distances and with similar magnitude could contribute (Albarello, 2012).

SASHA code (D'Amico and Albarello, 2008) gives as output, for each site analysed, the list of events contributing to the I_{REF} determination and the associated probability. As explained in Albarello (2012), these values can be represented in a disaggregation matrix, where for each bin of magnitude and distance, the normalized sum of the probability in the bin is reported. The earthquake corresponding to the maximum value of the paired distance/magnitude can be assumed to be the most "representative" event in the hazard estimation.

In this study, the probability values of I_{REF} were binned into classes of epicentral distances (2 km) and magnitude (0.25 unit). The probability values for each earthquake are summed up in the associated distance/magnitude bins, and normalized to provide the disaggregation of data (Figure 39).

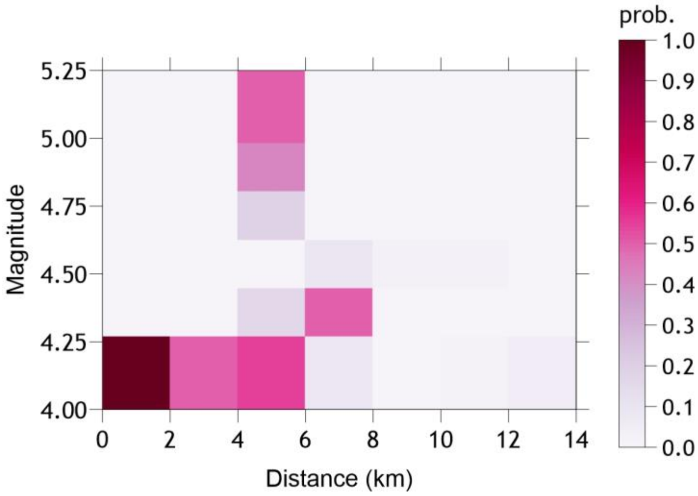

Figure 39. Disaggregation of moment magnitude (bin 0.25) versus epicentral distance for the village of Zafferana on Etna's eastern flank.

The hazard for Zafferana Etnea (I_{ref} = VII) is mainly due to small earthquakes (M_W 4.00-4.25) very close to the site (up to 6 kilometres away). Conversely, stronger earthquakes of the lower eastern flank contribute less to the hazard assessment. In the seismic history of the village, the earthquake which greatly contributes to the hazard occurred on October 19th, 1984.

1.3.5. Seismic scenario

Following the results obtained by the disaggregation analysis, the seismic scenario was calculated using the parameters of the 1984 Zafferana Etnea earthquake. The moment magnitude M_W used for the scenario is 4.2, which is equivalent to an epicentral intensity I_0 = VII EMS (Azzaro et al., 2011).

The scenario was calculated in terms of expected intensity at site I_S, in EMS scale. The intensity at site I_S, and correspondingly, the decay $\Delta I = I_0 - I_S$, are considered as binomial distributed random variables of a Bayesian model using a beta distributed random variable; the α and β hyperparameters include the prior information on the phenomenon. The mode of the smoothed binomial distribution is taken as an estimate of the intensity at site I_S; moreover, through the posterior distribution of the parameters, the Bayesian paradigm also provides rational measures of the parameter uncertainties.

A detailed description of the method used is described in Meroni et al. (2016), Azzaro et al. (2013b) and Rotondi et al. (2016).

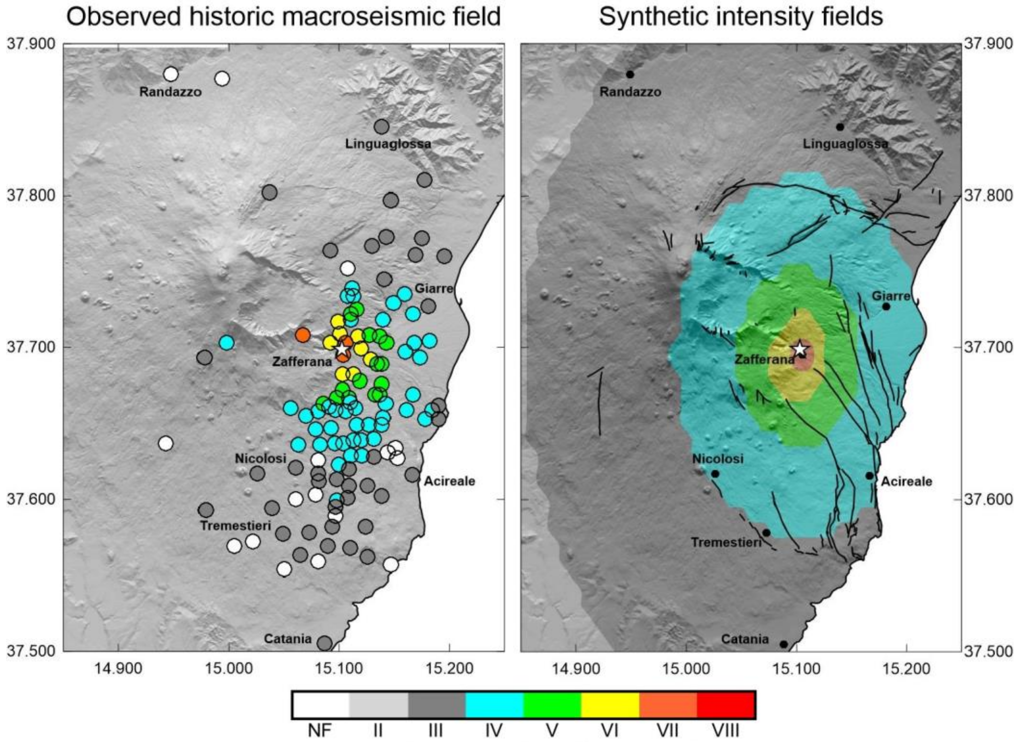

Figure 40. Left: Maps of the observed intensities of the 1984, October 19th earthquake, used as reference event. Right: seismic scenario in terms of synthetic intensity field (I_0 = VII EMS; M_W = 4.2).

Figure 40 shows the macroseismic intensities observed at sites for the 1984, October 19th earthquake (left), compared with the intensities estimated for the scenario (right). The colour of I_S assigned with uncertainties (like "VI-VII" or "IV-V", for example) are referred to the greater intensity value. The scenario well represents the observed data, especially for higher EMS values. Major variability concerns the extension of IV degree, which can be explained taking into account that in a macroseismic survey the elements to assess lower degrees are more subjective. Moreover, it should be noted that IV EMS does not imply the presence of damage.

1.3.6. Definition of Ground Motion scenarios for the town of Zafferana

Zafferana Etnea has been hit by various earthquakes occurring on Mt. Etna (Figure 41). In the last 200 years the maximum intensity felt in the area reached degree VII EMS, and several times degrees of VI-VII or VI. In general damaging earthquakes on Mt Etna are of relatively small magnitude but – as they occur very close to the surface – entail a considerable risk in the vicinity of the epicenter.

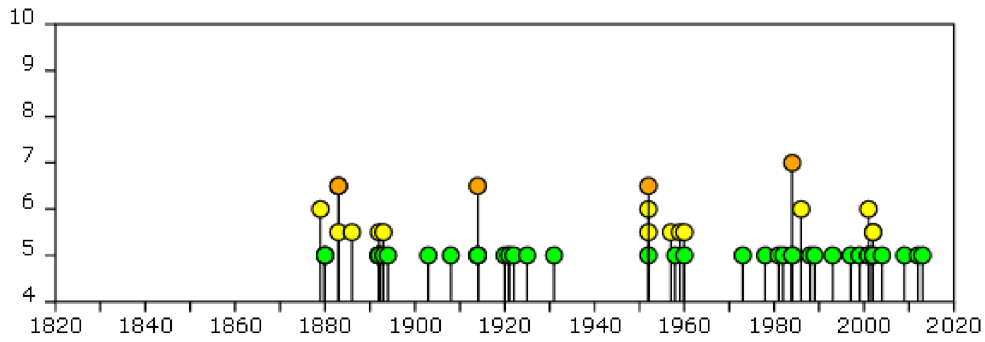

Figure 41. Seismic history of Zafferana in the last 200 years (from CMTE Working Group, 2014, http://www.ct.ingv.it/macro/etna/html_index.php.)

From the distribution of seismic events around Zafferana (Figure 46) we may identify two relevant scenarios (Table 68): 1) seismic events with Zafferana falling in the epicenter zone, 2) events occurring at some epicentral distance (5-10 km):

Table 8 – Scenario earthquakes for the test site Zafferana.

Earthquake	Epicentral intensity I_0 (EMS)	Magnitude M_w
Scenario 1		
1984, Oct 19	VII	4.2
2001, Jan. 09	VI	3.7
Scenario 2		
1879, Jun 17	VIII-IX	4.6
1914, May 08	IX-X	5.2
2002, Oct 29	VIII	4.8

Synthetic simulations of ground motion scenarios are based on the code Exsim (Boore, 2009) with slight modifications (see Langer et al., 2015). First simulations carried out so far regard an earthquakes M 3.5 close to the site and a further one, M 5 at a distance of ca. 7 km. Parameters were chosen following Langer et al. (2015).

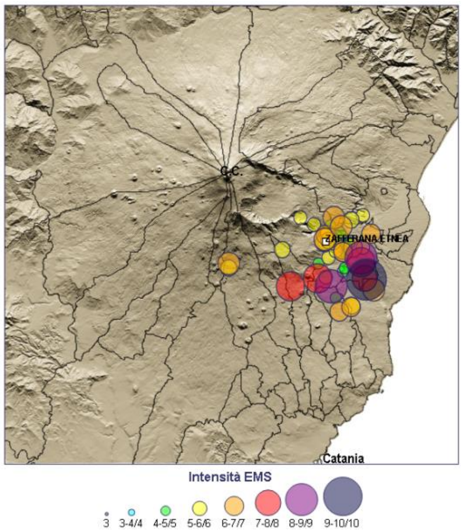

Figure 42. Seismic sources relevant for ground shaking at Zafferana (from CMTE Working Group, 2014, http://www.ct.ingv.it/macro/etna/html_index.php.)

Two types of sites were considered (Table *6*9). For the hardrock site no specific amplification factors were applied. Besides we also considered site amplifications for a D-type soil applying the functions given in Scarfi et al. (2016, see also Langer et al., 2015). are shown in.

Table 9 – Simulated ground motion parameters for both scenarios.

Event M 3.5, epicenter	PGA (gal)	PGV (cm/s)	IH (cm)
Site H	6.5	0.4	1.5
Site D	65	4.4	19
Event M 5, dist. = 7 km	**PGA (gal)**	**PGV (cm/s)**	**IH (cm)**
Site H	11	1	8
Site D	58	8	67

Figure **43** gives samples of response spectra obtained from the above ground motion parameters.

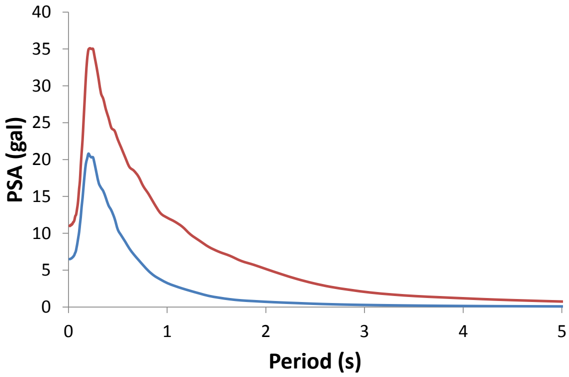

Figure **43**. Response spectra for "Hardrock". Blue: M 3.5, epicentre. Red: M 5, d=7 km.

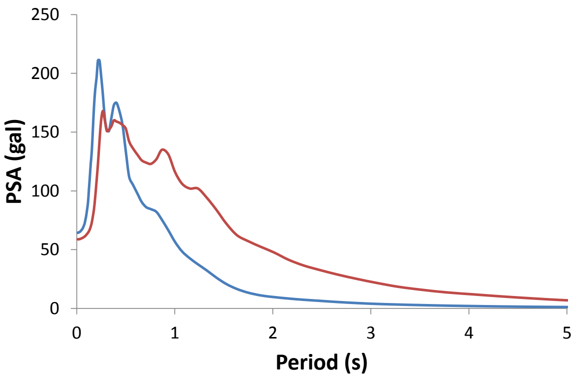

Figure **44**. Response spectra for "Soft Soil". Blue: M 3.5, epicentre. Red: M 5, d=7 km.

1.4 SEISMIC SCENARIOS FOR SOUTH ICELAND AREA

1.4.1. Introduction

Iceland is seismically very active, and has experienced many moderate to large earthquakes. Seismicity in Iceland is due to tectonic earthquakes originating near the rift between the Eurasian and the North-American plates, commonly known as the Mid-Atlantic ridge, as well as those due to volcanic activities. Tectonic earthquakes are less frequent and more damaging, while small volcanic earthquakes which cause no physical damage are frequently felt.

1.4.2. Seismotectonics

Most of seismic activity in Iceland is related to the Mid-Atlantic Ridge (MR), a divergent boundary in the North Atlantic Ocean between the North American and the Eurasian Plates (see Figure 45). A hotspot under the Vatnajökull glacier in eastern Iceland bends the MR eastward (Einarsson 1991). Interaction of the hotspot with the MR has created complex fracture zones—Tjörnes Fracture Zone (TFZ) in the north and South Iceland Seismic Zone (SISZ) in the south. Most of the destructive earthquakes in Iceland have occurred in these fracture zones. The MR enters Iceland at the tip of Reykjanes peninsula and continues eastwards creating a transition zone between Reykjanes Ridge to the west and Western Volcanic Zone (WVZ) and SISZ to the east. The seismic zone is narrow, <2 km wide in most places (Klein et al. 1977). Earthquakes in this zone are smaller than those in the SISZ.

The SISZ connects two sub-parallel rift zones, the WVZ and the Eastern Volcanic Zone (EVZ), forming a 10–15 km wide, east–west oriented, 60–70 km long fracture zone. This zone has produced many destructive seismic events, the latest being the 2008 M_w 6.3 Ölfus earthquake (Sigbjörnsson et al. 2009). Earthquakes of size as large as magnitude 7 can be expected in SISZ (Halldórsson 1992). Major earthquakes in this zone occur as sequences affecting the whole zone and lasting from a few days to years. In terms of exposure to seismic hazard, SISZ crosses south lowland with high population density compared to the rest of the country. This area accommodates many farms and small towns. It also contains many important critical infrastructures such as hydropower plants, geothermal power plants, and transportation network. SISZ is the pilot study area of Iceland in this project.

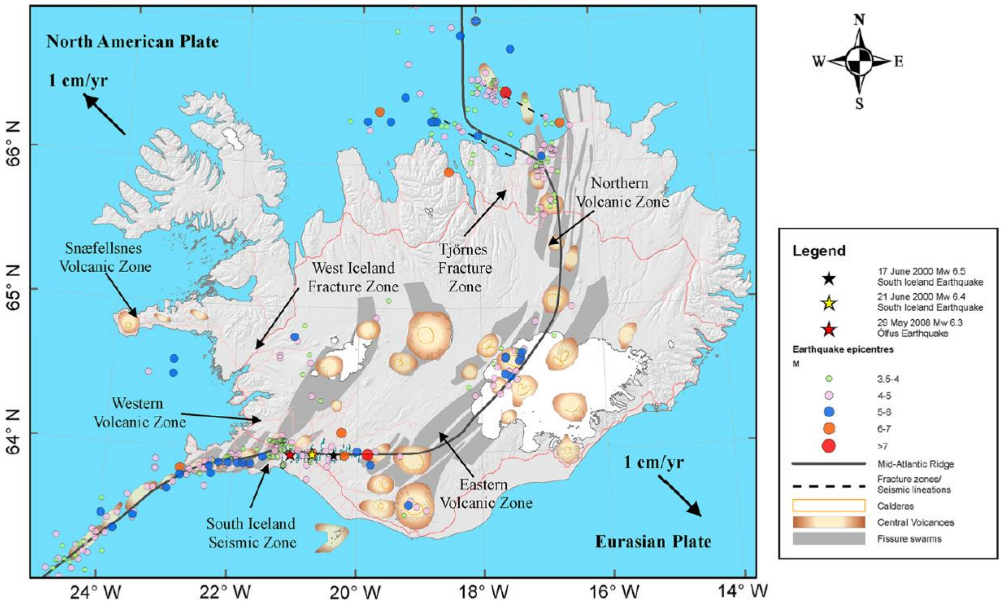

Figure 45. Seismotectonics of Iceland showing the Mid-Atlantic ridge, the major rifts and fracture zones. Epicentres of recorded earthquakes are marked with coloured circles, as indicated in the legend. The epicentres of the three recent earthquakes are marked with stars as indicated in the legend.

1.4.3. Seismic catalogue

Accounts of earthquakes in Iceland are available in historical archives since its settlement in the ninth century. The first documented earthquake is an event that occurred in 1164 in SISZ. An overview of the most important seismic events between 1200 and early 1400 is available in contemporary annals and archives. Information on earthquakes ceases to exist from 1430 for more than a century, but resumes after mid-sixteenth century. Estimates of earthquake size in Iceland based on teleseismic instrumental data are available since 1896. Magnitude estimates before instrumental data became available are based on the extension of damaged areas and observed spatial attenuation of damage (Halldórsson 1992). A parametric seismic catalogue of Iceland covering historical and recorded earthquakes (since 1986) was compiled by Ambraseys and Sigbjörnsson (2000). Since 1926, the Icelandic Meteorological Office (IMO) has compiled earthquake catalogue based on instrumental measurements from their SIL seismic network. For the Icelandic region, the recent European earthquake catalogue SHEEC (Grunthal et al. 2013), released by the SHARE project, is based on the catalogue of Ambraseys and Sigbjörnsson (2000) and that of IMO. D'Amico et al. (2016) extended and slightly modified the SHEEC catalogue for Iceland based on observations from Ambraseys and Sigbjörnsson (2000) and Sigbjörnsson and Rupakhety (2014). The resulting catalogue includes 896 earthquakes with M_w ranging from 4 to 7.1 that occurred from 1706 to 2008 (Figure 46).

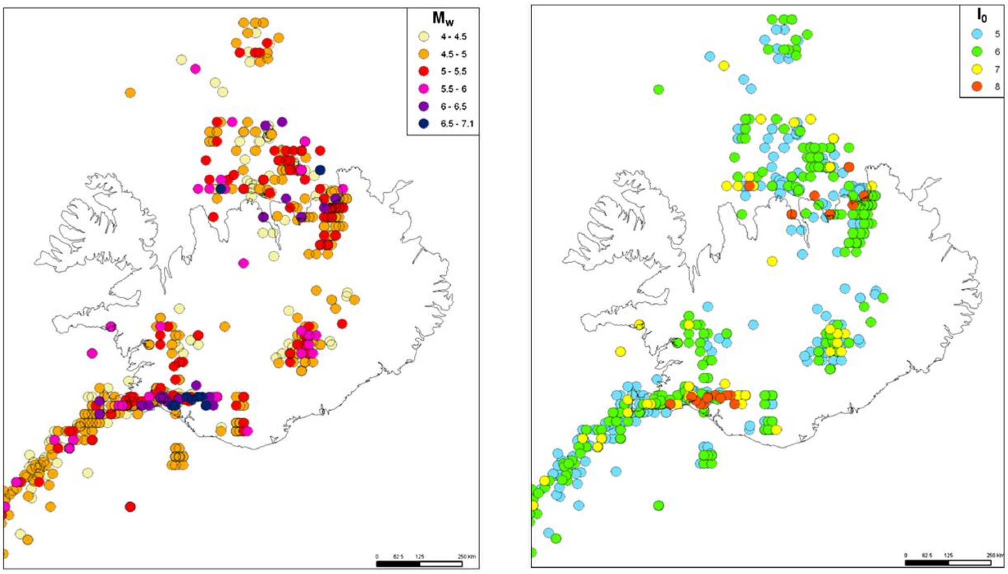

Figure 46. Earthquake catalogue of Iceland in terms of M_W (left) and epicentral macroseismic intensity I_0 (right).

The distribution of earthquakes shown in Figure 46 indicates that in terms of felt effects, SISZ and TFZ are the most critical areas in Iceland. Since SISZ is more densely populated and earthquake ground motion data are more abundant in this region, the case study region for Iceland is selected as SISZ. This is also due to the fact that recent strong earthquakes in the region have made damage data available, which is valuable in understanding vulnerability and risk due to non-structural elements.

1.4.4. Probabilistic seismic hazard in Iceland

Estimation of seismic hazard in Iceland has been an active research field for a few decades. Early efforts were focused on producing iso-acceleration and iso-intensity maps based on observations from past earthquakes (see, e.g., Halldórsson 1992). Probabilistic seismic hazard map corresponding to 0.2% annual probability of exceedance of horizontal peak ground acceleration (PGA) was prepared by Sigbjörnsson and Baldvinsson (1992). After the south Iceland earthquakes of 2000, additional data required for calibration of empirical ground-motion prediction equations (GMPEs) in Iceland became available and more detailed studies on probabilistic seismic hazard assessment (PSHA) using instrumental ground-motion measures followed. Solnes et al. (2004) used a simulated parametric catalogue and a locally calibrated GMPE based on Brune's source spectrum to compute 475-year return period hazard map for horizontal PGA (Figure 47a).

More recently, new hazard estimates for Iceland have been provided for several return periods in the frame of the EU project SHARE (http://www.share-eu.org/node/6, Giardini et al. 2013; Woessner et al. 2015). The map for PGA with 10 % probability of exceedance in 50 years (Fig. 2b, data downloaded from http://www.efehr.org:8080/jetspeed/portal/hazard.psml, Giardini et al. 2013) shows significant differences to the map of Solnes et al. (2004), due to the different earthquake catalogues, source models and attenuation relationships considered in the two studies, and hazard estimates by SHARE are higher in most areas, except in the eastern part of SISZ, where it predicts slightly lower hazard. The hazard map from SHARE seems to consider contributions of volcanic earthquakes more than that done by Solnes et al. (2004).

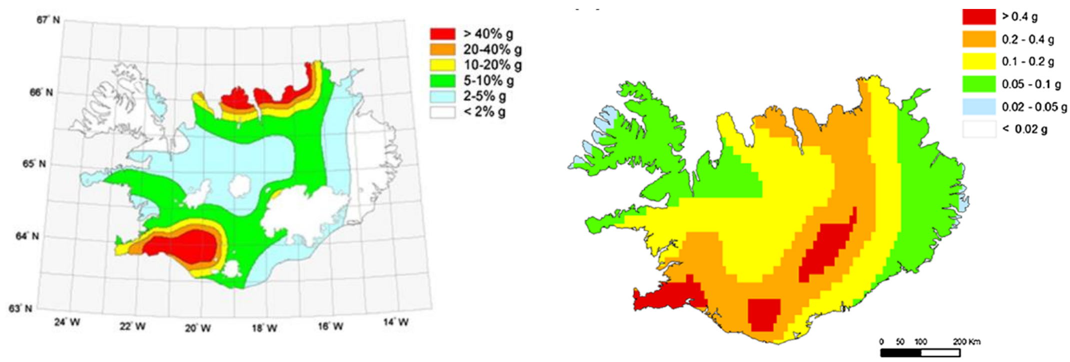

Figure 47. Probabilistic seismic hazard map of Iceland. Left: from Solnes et al. (2004); right: from SHARE project.

1.4.5. Hazard level relevant for non-structural damage mitigation

Modern seismic design codes place more emphasis on life safety performance level by avoiding collapse. Although performance based seismic design is gaining popularity in research, the current design code for seismic resistance in Europe, EC8, does not fully incorporate principles of performance based design directly. It, however, address some aspects of this philosophy by defining multiple performance requirements, which are:

1. No-collapse (or life safety) performance level. This level is intended for life safety in case of rare events. During such events, the structure as a whole and its load bearing elements should preserve their integrity and residual load bearing capacity. The

typical hazard level for this performance level for ordinary structures is defined by 475 years mean return period, or 10% probability of exceedance in 50-year reference period.

2. Damage limitation performance level. This level is intended for reduction in property loss due structural and non-structural elements due to more frequent earthquakes. This level is achieved by limiting the overall deformations (lateral displacements) of the structure to levels acceptable for the integrity of all its parts (including non-structural ones) and through (non-engineered) measures for the integrity of (masonry) infills. Typical hazard level for this performance level is 10% probability of exceedance in 10-year reference period or a mean return period of 95 years.

In addition, capacity design provisions are introduced in EC8 to prevent global collapse during very rare (maximum credible) earthquakes. In such cases, although immediate global collapse is prevented, damage beyond reparability is accepted.

What is lacking in the modern design codes is a more systematic provision for control of damage caused by building contents. Although some regulations exist for heavy machinery and equipment, no clear guidelines for safety of common household appliances are provided. Although damage limitation performance level, assures, to a certain degree, limitation of financial loss due to frequent earthquakes, it does not properly address the issue of injuries or potential casualties caused by loose objects inside buildings. There is a general lack of research regarding what threshold intensity should be used to control damages to and due to building contents during frequent earthquakes. At the same time, it is inevitable that damage limitation and life safety performance levels will most likely result in significant movement of building contents, resulting in injuries and financial loss. The unanswered question then is what level of hazard is suitable for design of anchors and connections for securing building contents. The answer to this question is not straight-forward, but depends on local construction practice as well as socio-economic conditions of the area affected by earthquakes. There are two main considerations that need attention. As a first alternative, buildings contents can be secured to withstand hazard level corresponding to life safety performance level. This is justified also by the fact that building contents pose threat to life either by impact or by blocking escape routes. Since anchoring of contents is not heavily costly, a 475-year mean return period level hazard would be appropriate in this alternative. The other alternative is that building contents are secured to withstand 95-year mean return period hazard. The drawback with this alternative is that considerable financial and economic loss may be expected in areas where moderate to strong earthquakes occur frequently. It should, however, be distinguished between non-structural elements that pose threat of injury or death, or those that are mainly associated with functional and financial loss. The latter categories may be designed for 95-year mean return period, except in critical facilities where immediate occupancy after an earthquake is crucial.

1.4.6. Seismic scenario for SISZ

The discussion above highlights the challenge of selecting a suitable scenario for non-structural damage. It was also indicated that this selection partly depends on building practice. For example, wind load requirements in Iceland are so stringent that most of the buildings safely withstand very high level of ground acceleration during earthquake without much structural damage. The experience from the three recent earthquakes, the two in June 2000 and one in May 2008 have shown that, even in areas which experienced ground shaking twice the level of prevalent seismic design requirements, structural damage was negligible compared to non-structural damage (see Bessason and Bjarnason 2016; Rupakhety et al. 2016). However, significant non-structural damage was suffered. In addition, damaging earthquakes in SISZ happen in sequences and are often of similar size (M_w 6.3-6.5), although larger earthquakes can be expected in the eastern part of SISZ. In this context, for the SISZ area, a suitable scenario earthquake is the one that corresponds to life safety performance level. In other words, deaggregation of 475-year hazard level can shed light on the most relevant scenario.

De-aggregation of seismic hazard in past studies (Solnes et al. 2004, D'Amico et al., 2016) show that earthquakes of M_w 6.3 within 5 to 15 km epicentral distance are the most significant contributors of 475-year return period hazard in SISZ (see Figure 48).

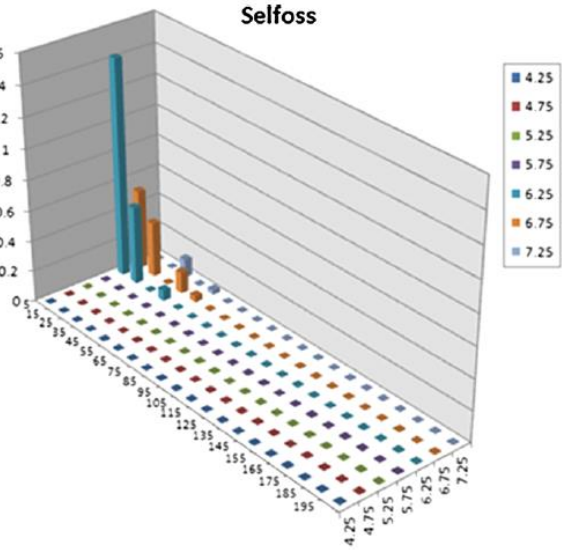

Figure 48. De-aggregation of 475 year mean return period hazard in Selfoss, located in SISZ. Colours in the legend indicate the moment magnitude M_W.

The three recent events - namely the 17 June 2000 M_W 6.5 earthquake, the 21 June 2000 M_W 6.4 earthquake, and the 29 May 2008 M_W 6.3 earthquake (see Figure 40) - fall within the expected scenario obtained from hazard de-aggregation. Ground motion data from these earthquakes are well recorded in SISZ (see Sigbjörnsson et al. 2009; Sigbjörnsson et al. 2007). Figure 49 shows the locations of the accelerometric stations of the Icelandic Strong Motion Network (ICESMN) which have recorded all three of these earthquakes. Three component ground acceleration time series are available at these stations, which allow for a very detailed description of ground motion hazard. In addition, it allows for computation of different ground motion intensity parameters, such as drift spectra, to evaluate the most suitable intensity measure to describe non-structural damage, which is the main aim of Task B2. As is can be seen from Figure 49, the SISZ is well covered by the ICESMN stations. Ground motion data as well as macroseismic data from these earthquakes have been collected and processed. In addition, peak ground motion intensities at locations where damage data is available, have already been simulated in this task using empirical scaling laws. The next step involves simulation of complete time histories at various locations in the study area in order to derive other intensity measures such as drift and floor spectra, and to study their correlation with observed damage. Based on such correlations, appropriate vulnerability models may be calibrated, which allows us to create risk map for the area, which is the main focus of Task B3 of this project. In the last part of this deliverable, distribution of ground motion intensity parameters using both recorded and simulated data for the three scenario earthquakes mentioned above, are presented.

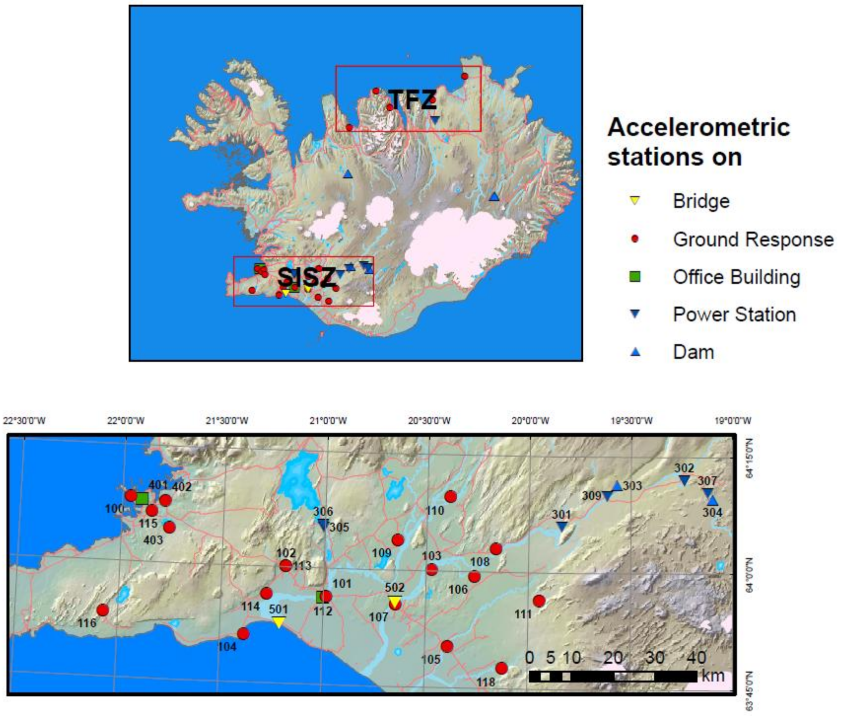

Figure 49. Active stations of the Icelandic Strong Motion Network (ICESMN).

An example of such results is presented in Figure 50, which shows the macroseismic intensity distribution in the study area obtained from survey data after the June 2000 earthquakes. These maps with other ground motion intensity parameters are also presented.

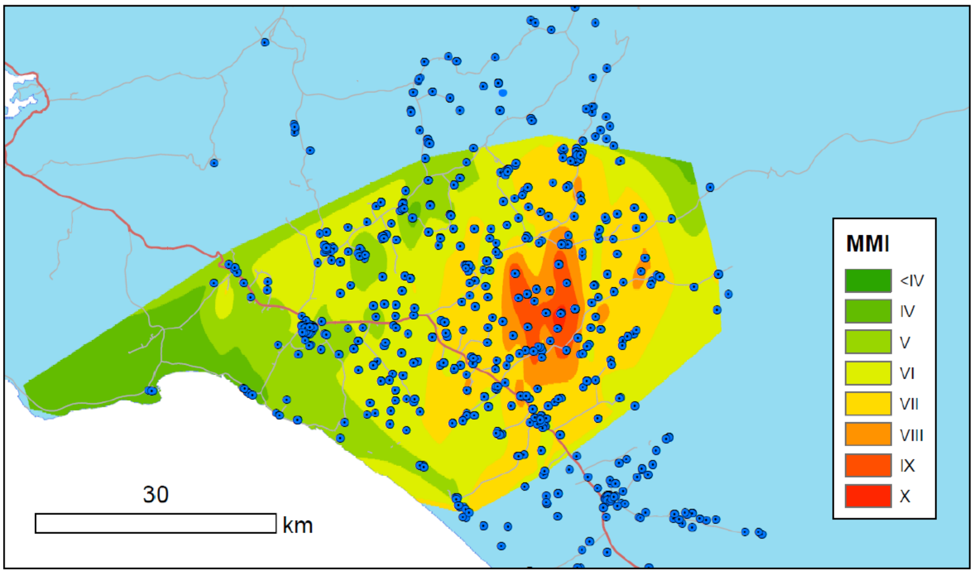

Figure 50. Macroseismic intensity (MMI) in the SISZ study area after the June 2000 South Iceland earthquakes.

1.4.7. Simulation of ground motion time histories

This section describes the ground motion simulation method, the resulting time histories, and scenario hazard maps based on the simulations.

Simulation method

Applying the stochastic finite fault simulation program EXSIM (see Beresnev and Atkinson 1990; Boore 2003, Motazedian and Atkinson 2005), the two earthquakes in June 2000 in South Iceland are modelled and used for simulation of ground motion records. A grid of 891 points was simulated, approximately covering the area where property damage occurred during these earthquakes. Determination of the model parameters (Table *6*10) are mostly based on the work of Ólafsson et al. (1998, 2014) and Ólafsson and Rupakhety (2017). The two earthquakes have strike slip mechanisms and occurred at shallow depth on near vertical faults. High acceleration values (~80%g) were observed in the near-field and attenuated rapidly with distance from the fault, with a R^2 rate of attenuation. A larger stress-drop of 140 bar was used for the 17th June earthquake vs. 100 bar for the stress drop for the 21st June event.

Table 10 – EXSIM parameters for simulations of the June 17th and 21st earthquakes in 2000.

Parameter	Values
Moment magnitude, M_w	6.5
Source mechanism	Strike-slip
Fault parameters	Strike: 0.5° , Dip: 90°
Fault dimension (km^2)	11x10
Depth to the top (km)	0.5
Stress drop (bar)	140
Average S-wave velocity (km/s)	3.6
Attenuation parameter, Q	500 (constant)
Geometric spreading	R<= 30 km: R^{-2} , R>30 km: R^{-1} R_{ref}= 3.2 km
Density (g/cm^2)	2.8
Site effects	Not applied (most sites are classified as rock or stiff soil)
Spectral decay parameter, [illegible]s[illegible]	0.04
Ground motion duration (s)	T = 1.85(r/[illegible]) + $0.008d^{1.78}$ (R,T) = (0,2s),(40km,7s),(100km, 26s)
Fault segment size, dw x dl	2 km x 2 km
Number of simulations	5

Comparison with recorded data

This section validates the simulated time series by comparing them with recorded data. Ground motion parameters at recording stations and the closest simulation stations are compared for validation.

Comparison of recorded and simulated PGA values are shown in Table 11. While the simulated PGA match the recorded ones reasonably well at some stations, there are large differences at some stations. Recorded PGA is known to show a large variability within a small area, a feature not captured by simulations.

Table 11 – Comparison of recorded and simulated PGA.

Station	17 June Event, PGA (g)	21 June Event, PGA (g)

Number				
	Recorded	Simulated	Recorded	Simulated
111	0.28	0.10	-	0.03
108	0.16	0.20	-	0.04
106	0.34	0.46	0.05	0.05
105	0.48	0.20	0.17	0.06
103	0.63	0.44	0.40	0.17
502	0.53	0.23	-	0.53
109	0.38	0.13	0.70	0.28
305	0.04	0.04	0.11	0.08
112	0.07	0.05	0.13	0.15
113	0.11	0.04	0.12	0.06
104	0.07	0.03	0.11	0.03
107	-	0.22	0.56	0.53

The attenuation of PGA with distance is shown in Figure 51. These figures compare the attenuation of simulated and recorded PGA values. For comparison, attenuation model based on a point source model (see Ólafsson and Rupakhety, 2017) are also shown. The median attenuation model is shown with the solid line while the dashed lines represent plus/minus one standard deviation estimates. The simulated PGA values show similar attenuation patterns as the recorded PGA values. Attenuation of simulated PGV is compared to that of recorded data in Figure 52.

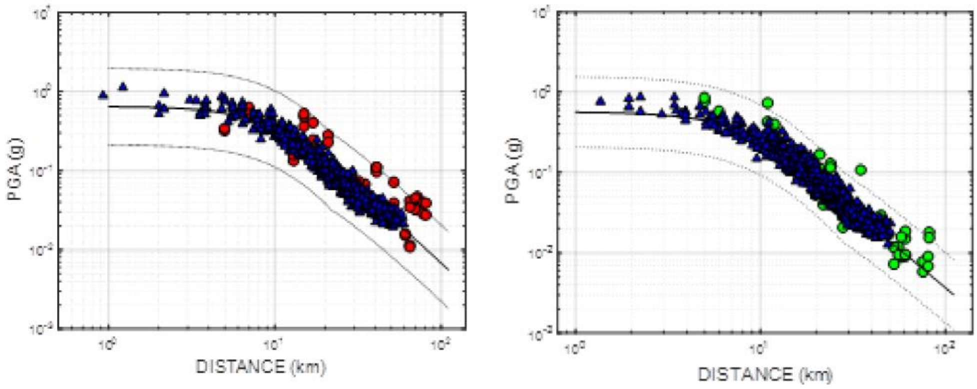

Figure 53. PGA as a function of epicentral distance, from simulations (blue triangles) dots represent PGA from recordings of a) 17th June 2000. and b) 21st June 2000 earthquakes.

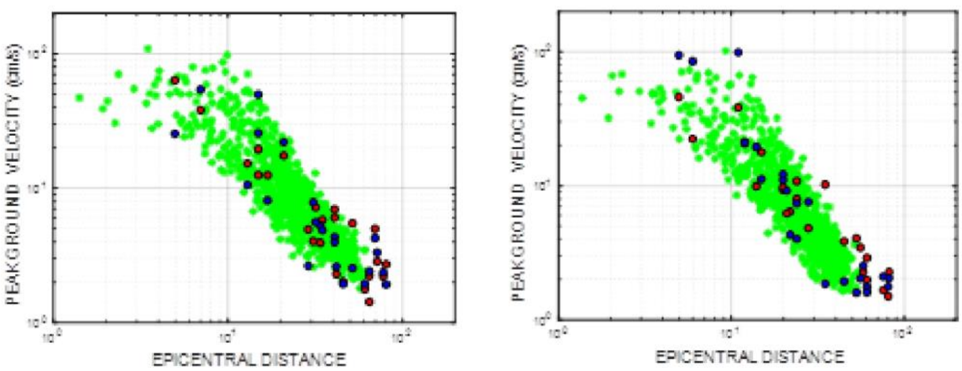

Figure 542. Attenuation of PGV with distance. Green points are PGV values from simulated records and the red and blue dots are PGV values obtained from measurements in the two earthquakes: a) Earthquake of 17th June 2000 b) Earthquake of 21st June 2000.

Simulated ground motion intensity (PGA)

Distribution of PGA obtained from simulated motions are shown in Figure 553 and 564. respectively, for the 17th and 21st June 2000 earthquakes. Damages caused by these earthquakes were recorded after the 21st June event. Therefore, the damage can be considered to be caused by the larger ground motion intensity of the two events, which is shown in Figure 55. Accumulation of damage between the events likely happened, but cannot be modelled by available data. The results indicate intense shaking in the epicentral area, which is comparable to what was recorded during the earthquakes.

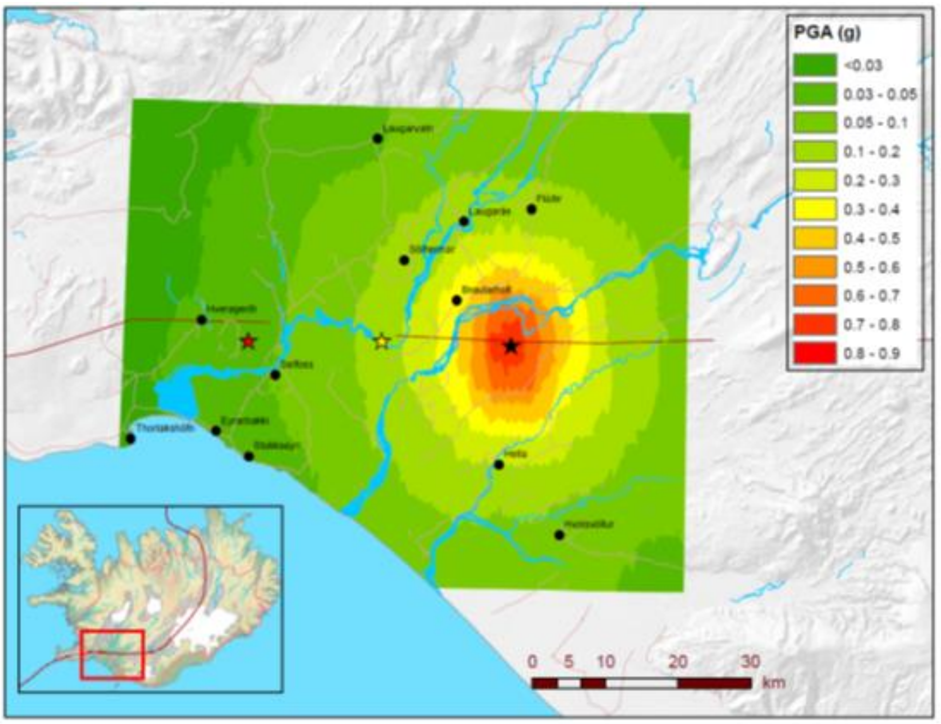

Figure 573. Distribution of PGA in the study area. The PGA values correspond to simulated ground motion for the 17 June 2000 M_w 6.5 earthquake.

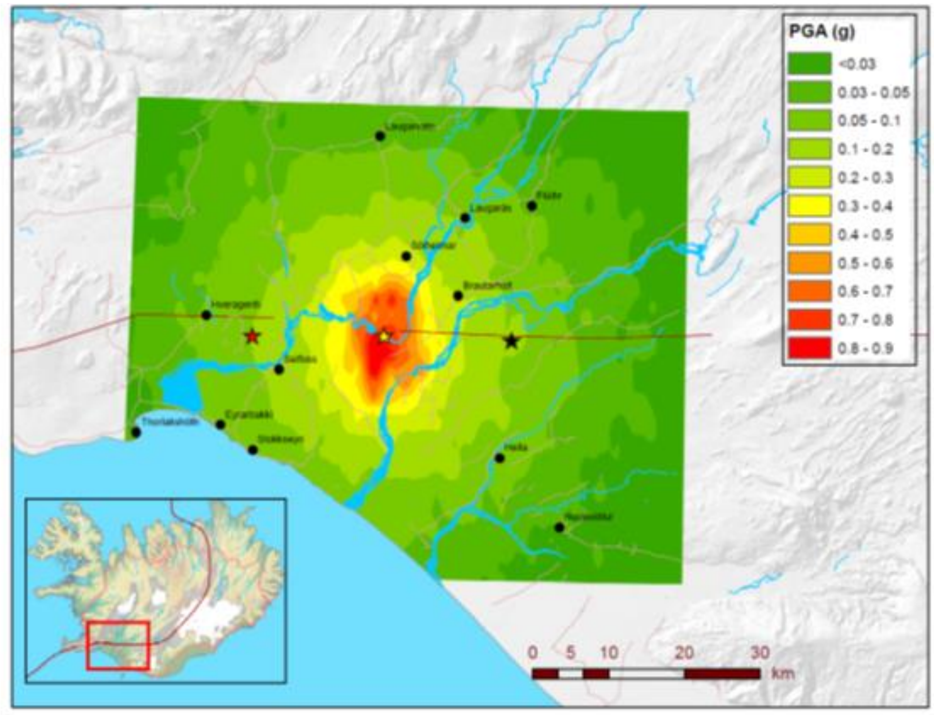

Figure 584. Same as in Figure 53, but for 21st June 2000 Mw 6.5 earthquake.

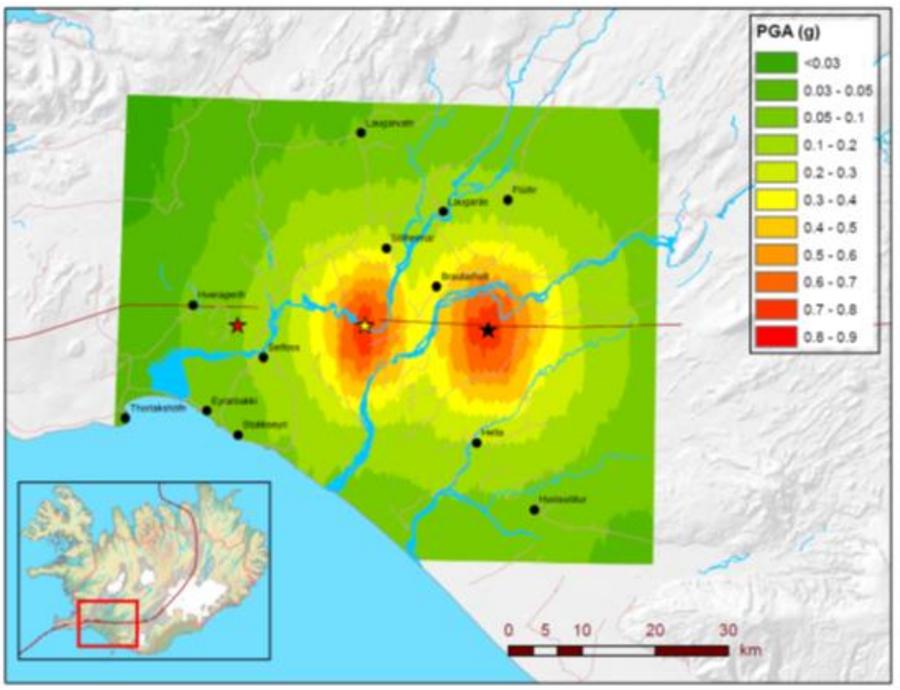

Figure 595. Distribution of PGA in the study area. Larger PGA from the 17th and 21st June 2000 earthquakes is considered.

As discussed in deliverable B2, some non-structural elements are more sensitive to structural drift rather than peak ground acceleration. The simulated time series allow computation of drift spectrum in the study area. Since most of the buildings in the study area are short and stiff, maximum drift of structures with vibration period less than 0.5s is considered here. The maximum drifts due to the 17 and 21 June earthquakes are shown in Figures 56 and 57 respectively. The larger drift at different locations due to these two earthquakes is shown in Figure 58. The results indicate severe drift demand on structures in the epicentral area. Close to the epicentres, the drift demand is as large as 2%. Such high levels of drift would cause structural damage to buildings. However, structural damage during these earthquakes was not significant, even in the epicentral region. The region for this is that the buildings in the area are very stiff and unlikely to have vibration period as long as 0.5s. Had there been such flexible buildings, life safety performance levels would have been exceeded during these earthquakes. Eurocode 8 sets a drift limit of 0.5% drift for brittle non-structural elements attached to the structure. This limit is exceeded in a wide area, as large as approximately 40km x 40km around the two earthquakes. Many towns and villages in the area lie in this region. As is predicted by the drift distribution, non-structural damage to brittle components attached to the structures was widespread in the area. For non-structural elements not interfering with the structure, the Eurocode 8 drift limit is 1%. The calculations show that this limit is exceeded in an area of about 20km x 20km around the two earthquakes. Widespread damage to such elements were observed during these earthquakes.

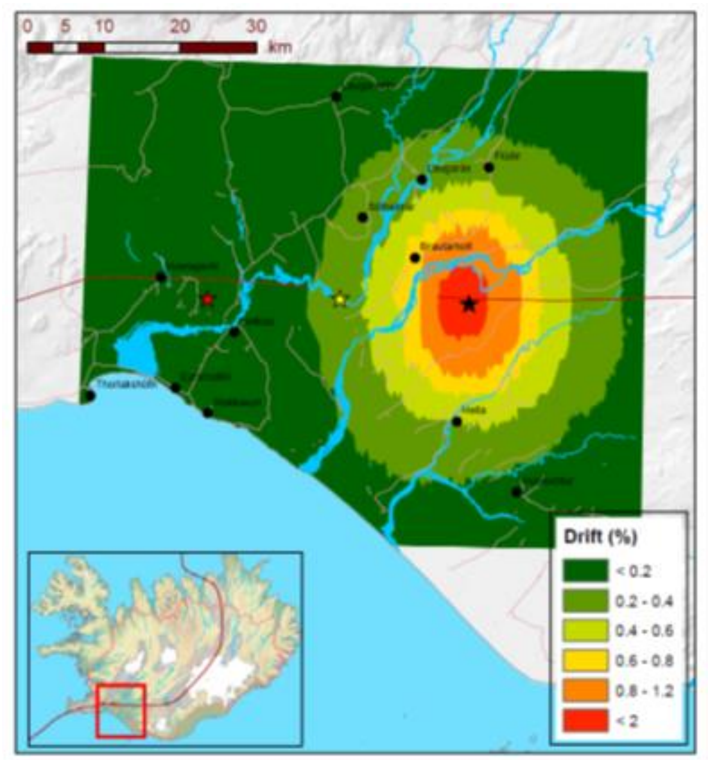

Figure 606. Spatial distribution of maximum interstory drift (natural period up to 0.5s) corresponding to ground motion generated by the 17 June 2000 earthquake.

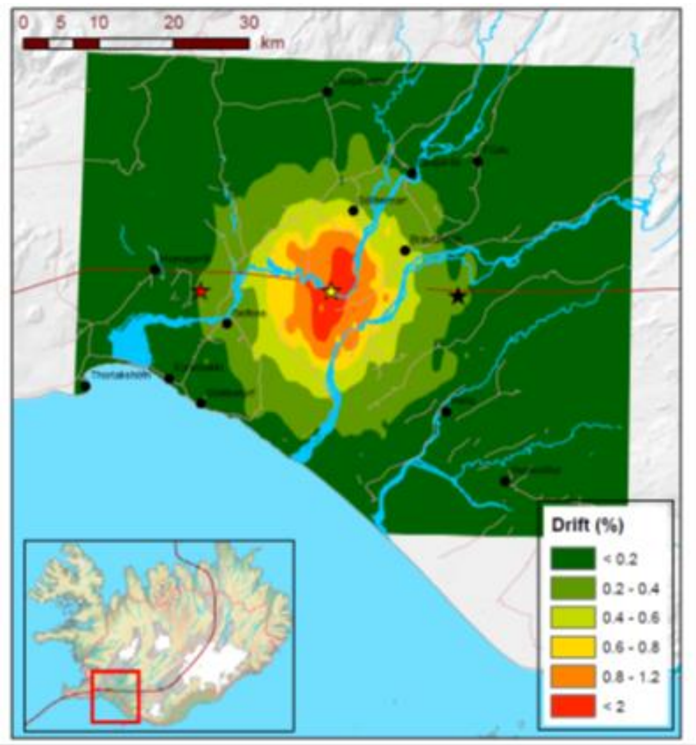

Figure 617. Same as in Figure 56 but for 21 June 2000 earthquake.

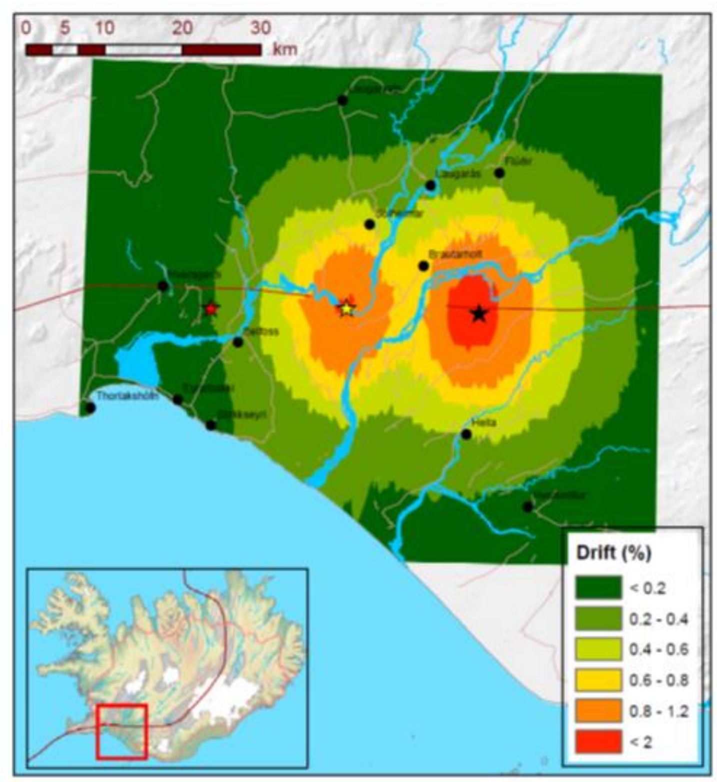

Figure 628. Same as in Figure 56 but for 21 June 2000 earthquake.

1.4.8. Conclusions

The seismically most affected area in Iceland is the SISZ which experiences many tectonic earthquakes originating near the MR. Since SISZ is also relatively densely populated with agricultural land, farms, transportation network and power plants, it was selected as the primary study site in this project. The selection of this site is also motivated by the availability of detailed ground motion and building damage data from past earthquakes.

Although modern seismic design codes try to indirectly control financial loss due to non-structural elements by referring a 95 year mean return period hazard, clear guidelines on prevention of financial loss and human injury due to movement of building contents, is lacking. Selection of a proper scenario for this performance requirement depends not only on the seismotectonics of the study area but also on the quality of constructions. Based on a detailed study of seismotectonics, probabilistic seismic hazard analysis and their de-aggregation, as well as damage pattern observed during recent earthquakes, it was decided that the June 2000 South Iceland earthquakes and the May 2008 Ölfus earthquake provide suitable scenario for the study area. Ground motion during this earthquake have been recorded by many stations of the ICESMN, and post-earthquake surveys have provided information on macroseismic effects. This task has completed a detailed study of literature, design code requirements, historical earthquakes, and their effects in the study area to decide on the suitable scenarios. In addition, compilation and processing of recorded ground motion as well as macroseismic data have been performed. Simulation using empirical ground motion prediction equations has been employed to estimate peak ground motion intensity measures at areas where instrumental data are not available. Since one of the aims of this project is to identify suitable ground motion intensity parameters for non-structural damage, peak ground motion intensity values are not sufficient. Drift spectra is expected to be a better intensity parameter. To estimate drift spectra, complete ground motion time histories are required. To achieve this task, ground motion time histories were simulated in a grid around the epicentres of the 17 June 2000 and 21 June 2000 earthquake scenarios. The simulated time series were used to compute drift spectra, and maximum drift for structures with fundamental period less than 0.5 were mapped. The results indicate very large drift demands on the structures. Drift demands as large as 2% were calculated close to the source. Such high drift demands would cause structural collapse of squat wall structures. However, structural damage was not extensive during these earthquakes. This indicates that the actual drift during the earthquakes was less than what is computed here. There are two potential reasons for this. The first is that the drift spectra are based on a period to height scaling equations that might not be suitable for the building stock in the area. The buildings in the study area are stiffer than implied by the commonly used period-height scaling equations. It is therefore important to conduct research studies to calibrate proper height-period equations for Icelandic buildings. The second explanation is that the maximum drifts presented here cover a period range of 0 to 0.5s. Most of the buildings in the study area have considerably lower vibration periods.

REFERENCES

Albarello, D. [2012] Design earthquake from site-oriented macroseismic hazard estimates, *Bollettino di Geofisica Teorica e Applicata*, Vol. 53, p.p. 7-18.

Albarello, D., Mucciarelli, M. [2002] Seismic hazard estimates using ill-defined macroseismic data at site, *Pure and Applied Geophysics*, Vol. 159, p.p. 1289-1304.

Alparone, S., Maiolino, V., Mostaccio, A., Scaltrito, A., Ursino, A., Barberi, G., D'Amico, S., Di Grazia, G., Giampiccolo, E., Musumeci, C., Scarfi, L., Zuccarello, L. [2015] Instrumental seismic catalogue of Mt. Etna earthquakes (Sicily, Italy): ten years (2000-2010) of instrumental recordings, *Annals of Geophysics*, Vol. 58, N. 4, pag. S0435

Ambraseys, N.N., Sigbjörnsson, R. [2000] Re-appraisal of the seismicity of Iceland, *Earthquake Engineering Research Centre*, University of Iceland, Selfoss.

Atkinson, G. M., & Boore, D. M. (2006). Earthquake Ground-Motion Prediction Equations for Eastern North America. Bulletin of the Seismological Society of America, 96(6), 2181-2205. doi: 10.1785/0120050245

Atkinson, G. M., & Boore, D. M. (2011). Modifications to Existing Ground-Motion Prediction Equations in Light of New Data. Bulletin of the Seismological Society of America, 101(3), 1121-1135. doi: 10.1785/0120100270

Azzaro, R. [2004] Seismicity and active tectonics in the Etna region: constraints for a seismotectonic model, in Bonaccorso, A., Calvari, S., Coltelli, M., Del Negro, C., Falsaperla, S. (eds.), *Mt. Etna: volcano laboratory*, American Geophysical Union, p.p. 205-220.

Azzaro, R., Barbano, M.S., D'Amico, S., Tuvè, T. [2006] The attenuation of seismic intensity in the Etna region and comparison with other Italian volcanic districts, *Annals of Geophysics*, Vol. 49, p.p. 1003-1020.

Azzaro, R., Barbano, M.S., D'Amico, S., Tuvè, T., Albarello, D., D'Amico, V. [2008] First studies of probabilistic seismic hazard assessment in the volcanic region of Mt. Etna (Southern Italy) by means of macroseismic intensities, *Bollettino di Geofisica Teorica e Applicata*, Vol. 49, p.p. 77-91.

Azzaro, R., Branca, S., Gwinner, K., Coltelli, M. [2012] The volcano-tectonic map of Etna volcano, 1:100.000 scale: morphotectonic analysis from high-resolution DEM integrated with geologic, active faulting and seismotectonic data. *Italian Journal of Geoscience (Boll. Soc. Geol. It.)*, Vol. 13, N. 1, p.p. 153–170, doi:10.3301/IJG.2011.29

Azzaro, R., Castelli, V., [2015] Materials for an earthquake catalogue of Mt. Etna volcano from 1600 to 1831. *Quaderni di Geofisica*, Vol. 123, 278 pp.

Azzaro, R., D'Amico, S., Tuvè, T. [2011] Estimating the magnitude of historic earthquakes from macroseismic intensity data: new relationships for the volcanic region of Mount Etna (Italy), Seismological Research Letters, Vol. 82, p.p. 533-544.

Azzaro, R., D'Amico, S., Peruzza, L., Tuvè, T. [2013a] Probabilistic seismic hazard at Mt. Etna (Italy): The contribution of local fault activity in mid-term assessment, *Journal of Volcanology and Geothermal Research*, Vol. 251, p.p. 158-169.

Azzaro, R., D'Amico, S., Rotondi, R., Tuvè, T., Zonno, G. [2013b] Forecasting seismic scenarios on Etna volcano (Italy) through probabilistic intensity attenuation models: A Bayesian approach. *Journal of Volcanology and Geothermal Research*, Vol. 251, p.p. 149-157.

Beresnev, I.A., Atkinson, G.M. [1998] FINSIM a FORTRAN program for simulating stochastic acceleration time histories from finite faults. *Seismological Research Letters*, Vol. 69 (1), p.p. 27-32.

Bessason, B., Bjarnasson, J. Ö. [2016] Seismic vulnerability of low-rise residential buildings based on damage data from three earthquakes (Mw 6.5, 6.5, 6.3), *Engineering Structures*, Vol. 111, p.p. 64-79.

Boore, D.M. [2003] Simulation of ground motion using the stochastic method. *Pure and applied geophysics*, Vol. 160 (3-4), p.p. 635-676

Boore, D.M. [2009] Comparing stochastic point-source and finite-source ground-motion simulations: SMSIM and EXSIM. *Bull. Seism. Soc. Am.*, Vol. 99, p.p. 3202–3216.

Carvalho, A. [2008] Leis de atenuação para Portugal Continental: Laboratório Nacional de Engenharia Civil (LNEC).1/2008-NESDE

Carvalho, A. [2009] Leis de atenuação semi-empíricas para Portugal Continental: LNEC, Laboratório Nacional de Engenharia Civil

CMTE Working Group [2014] Catalogo Macrosismico dei Terremoti Etnei, 1832–2013. *INGV Catania*. http://www.ct.ingv.it/macro/.

D'Amico, V., Albarello, D. [2008] SASHA: a computer program to assess seismic hazard from intensity data, *Seismological Research Letters*, Vol. 79, p.p. 663-671.

D'Amico, V., Albarello, D., Sigbjörnsson, R., Rupakhety, R. [2016] Seismic hazard assessment for Iceland in terms of macroseismic intensity using a site approach, *Bulletin of Earthquake Engineering*, Vol. 14, p.p. 1797-1811.

Einarsson, P. [1991] Earthquakes and present-day tectonism in Iceland, *Tectonophysics,* Vol. 189, p.p. 261–279.

Estêvão, J. M. C., & Oliveira, C. S. (2001). Parâmetros que Condicionam os Valores da Casualidade Sísmica. Paper presented at the SÍSMICA 2001 - 5º Encontro Nacional sobre Sismologia e EngenhariaSísmica, Açores: Laboratório Regional de Engenharia Civil.

Eurocódigo 8 - Projecto de estruturas para resistência aos sismos, Parte 1: Regras gerais, acções sismicas e regras para edificios, Anexo Nacional, EC8 NP EN 1998-1 (2010).

Giampiccolo, E., D'Amico, S., Patanè, D., Gresta, S., [2007] Attenuation and source parameters of shallow microearthquakes at Mt. Etna volcano (Italy). *Bulletin of the Seismological Society of America,* Vol. 97, N. 1B, p.p. 184-197.

Giardini, D., Woessner, J., Danciu, L., Crowley, H., Cotton, F., Grünthal, G., Pinho, R., Valensise, G., Akkar, S., Arvidsson, R., Basili, R., Cameelbeeck, T., Campos-Costa, A., Douglas, J., Demircioglu, M.B., Erdik, M., Fonseca, J., Glavatovic, B., Lindholm, C., Makropoulos, K., Meletti, C., Musson, R., Pitilakis, K., Sesetyan, K., Stromeyer, D., Stucchi, M., Rovida, A. [2013] Seismic hazard harmonization in Europe (SHARE): Online Data Resource., doi:10.12686/SED-00000001-SHARE.

Godano, C., & Arcangelis, L. d. (2014). Earthquakes temporal occurrence: a statistical study, from http://www.amra.unina.it/docs/PUBBLICAZIONI/cluster.pdf

Gomberg, J., Belardinelli, M. E., Cocco, M., & Reasenberg, P. [2005] Time-dependent earthquake probabilities. *Journalof Geophysical Research*, 10(B05D04). doi: 10.1029/2004JB003405

Grünthal, G., (eds.) [1998] European macroseismic scale 1998 (EMS-98). *European Seismological Commission, subcommission on Engineering Seismology, working Group Macroseismic Scales*. Conseil de l'Europe, Cahiers du Centre Européen de Géodynamique et de Séismologie, 15, Luxembourg, pp. 99. http://www.ecgs.lu/cahiers-bleus/.

Grünthal, G., Wahlström, R., Stromeyer, D. [2013] The SHARE European earthquake catalogue (SHEEC) for the time period 1900–2006 and its comparison to the European-Mediterranean earthquake catalogue (EMEC), *J Seismol*, Vol. 17, p.p. 1339–1344.

Halldórsson, P. [1992] Seismic hazard assessment based on historical data and seismic measurements, *International conference on preparedness and mitigation for natural disaster*, Iceland.

INE. [2011]. V Recenseamento Geral da Habitação: Instituto Nacional de Estatística.

Klein, F.W., Einarsson, P., Wyss, M. [1977] The Reykjanes Peninsula, Iceland, earthquake swarm of September 1972 and its tectonic significance, *J Geophys Res*, Vol. 82, p.p. 865–888.

Lagomarsino, S. [2006] Vulnerability Assessment of Historical Buildings. In C. S. Oliveira, A. Roca & X. Goula (Eds.), Assessing and Managing Earthquake Risk: Springer Science.

Langer, H., Tusa, G., Scarfi, L. [2015] Ground-motion scenarios on Mt. Etna inferred from empirical relations and synthetic simulations. *Bull. Earthquake Eng.*, DOI 10.1007/s10518-015-9823-1

McNutt, S.R., [2005] Volcanic seismology. *Annual Review of Earth and Planetary Sciences*, Vol. 32, p.p. 461-491.

Meroni, F., Zonno, G., Azzaro, R., D'Amico, S., Tuvè, T., Oliveira, C.S., Ferreira, M.A., Mota de Sá, F., Brambilla, C., Rotondi, R., Varini, E. [2016] The role of the urban system dysfunction in the assessment of seismic risk in the Mt. Etna area (Italy). *Bulletin of Earthquake Engineering*, Vol. 17, N. 7, p.p. 1979–2008, doi: 10.1007/s10518-015-9780-8.

Motazedian, D., Atkinson, G.M. [2005] Stochastic finite-fault modeling based on a dynamic corner frequency. *Bulletin of the Seismological Society of America*, Vol. 95 (3), p.p. 995-1010.

Mota de Sá, F. [2009] Desenvolvimento e implementação do Simulador Sísmico e de Tsunamis do Algarve.WP 22 Final Report.

Mota de Sá, F. [2016] Seismic Risk - New instruments for Analysis and Communication. Phd, University Of Lisbon, Lisbon.

Musson, R. M. W., Tsapanos, T. M., & Nakas, C. T. [2002] A Power-Law Function for Earthquake Interarrival Time and Magnitude. *Bulletin of the Seismological Society of America*, Vol. 92, No. 5, pp. 1783–1794, June 2002, 92(5), 1783-1794.

Ólafsson, S., Galluzzo, D., Carvalho, A., Langer, H., Oliveira, C., Sigbjörnsson, R. [2014] Ground motion modelling based on data from the Azores islands, Italy and South-Iceland. Proceedings of the Second European Conference on Earthquake Engineering and Seismology, Istanbul, Aug. 25-29.

Ólafsson, S., Rupakhety, R. [2017] Source parameters from acceleration records for earthquakes during the period 1987-2008 in South Iceland. 16th World Conference on Earthquake Engineering, 16WCEE 2017, Santiago Chile, January 9th to 13th 2017, Paper No. 4572.

Ólafsson, S., Sigbjörnsson, R., Einarsson, P. [1998] Estimation of source parameters and Q from acceleration recorded in the Vatnafjöll Earthquake in South Iceland. *Bulletin of the Seismological Society of America*, Vol. 88 (2), p.p. 556-563.

Petersen, M. D., Cao, T., Campbell, K., & Artur, D. [2007] Time-independent and Time-dependent Seismic Hazard Assessment for the State of California: Uniform California Earthquake Rupture Forecast Model 1.0. *Seismological Research Letters*, 78(1), 99.

Rotondi, R., Zonno, G., [2004] Bayesian analysis of a probability distribution for local intensity attenuation. *Annals of Geophysics*, Vol. 47, N. 5, p.p. 1521-1540.

Rotondi, R., Varini, E., Brambilla, C. [2016] Probabilistic modelling of macroseismic attenuation and forecast of damage scenarios. *Bulletin of Earthquake Engineering*, Vol. 14, N. 7, p.p. 1777-1796, doi:10.1007/s10518-015-9781-7

Rovelli, A., Bonamassa, O., Cocco, M., Di Bona, M., Mazza, S., [1988] Scaling laws and spectral parameters of the ground motion in active extensional areas in Italy. *Bulletin of the Seismological Society of America*, Vol. 78, p.p. 530-560.

Rupakhety, R., Olafsson, S., Sigbjörnsson, R. [2016] Damage to residential buildings in Hveragerði during the 2008 Ölfus Earthquake: simulated and surveyed results. *Bulletin of Earthquake Engineering*, Vol. 14 N. 7, p.p. 1945-1955.

Scarfì, L., Langer, H., Garcia-Fernandez, M., Jimenez, J. M. [2016] Path effects and local elastic site amplification: two case studies on Mt Etna (Italy) and Vega Baja (SE Spain). *Bull. Earthquake Eng.*, DOI 10.1007/s10518-016-9883-x

Sigbjörnsson, R., Baldvinsson, G.I. [1992] Seismic hazard and recordings of strong ground motion in Iceland. In: *Proceedings of the 10th world conference on earthquake engineering*, Rotterdam, The Netherlands, Vol. 1, p.p. 419–424.

Sigbjörnsson, R., Olafsson, S., Snæbjornsson, J.Th. [2007] Macroseismic effects related to strong ground motion: a study of the South Iceland earthquakes in June 2000, *Bulletin of Earthquake Engineering*, Vol. 5, N. 4, p.p. 591-608.

Sigbjörnsson, R., Rupakhety, R. [2014] A saga of the 1896 South Iceland Earthquake: magnitudes, macroseismic effects and damage, *Bulletin of Earthquake Engineering*, Vol. 12, N. 1, p.p. 171-184.

Sigbjörnsson, R., Snæbjörnsson, J.Th., Higgins, S.M., Halldórsson, B., Ólafsson, S. [2009] A note on the M6.3 earthquake in Iceland on 29 May 2008 at 15:45 UTC, *Bulletin of Earthquake Engineering*, Vol. 7, N. 1, p.p. 113–126.

Sigbjörnsson, R., Zonno, G., Oliveira, C.S. (eds), [2016] The European project UPStrat-MAFA: Urban Disaster Prevention Strategies Using MAcroseismic Fields and FAult Sources, *Bulletin of Earthquake Engineering*, Vol. 14, N. 7.

Vilanova, S. P., & Fonseca, J. F. B. D. [2004] A falha do Vale Inferior do Tejo na análise da perigosidade sísmica. Paper presented at the SÍSMICA 2004 - 6º Congresso Nacional de Sismologia e Engenharia Sísmica, Guimarães.

Wald, D.J., Quitoriano, V., Heaton, T.H., Kanamori, H., Scrivner, C.W., Worden, C.B., [1999] Trinet 'ShakeMaps': rapid generation of peak ground motion and intensity maps for earthquakes in southern California. *Earthquake Spectra*, Vol. 15, p.p. 537-555.

Woessner, J., Danciu, L., Giardini, D., Crowley, H., Cotton, F., Grünthal, G., Valensise, G., Arvidsson, R., Basili, R., Demircioglu, M.B., Hiemer, S., Meletti, C., Musson, R., Rovida, A., Sesetyan, K., Stucchi, M., the SHARE consortium [2015] The 2013 European Seismic hazard model: key components and results, *Bulletin of Earthquake Engineering*, doi:10.1007/s10518-015-9795-1.

Zonno, G., Rotondi, R., Brambilla, C., [2009] Mining macroseismic fields to estimate the probability distribution of the intensity at site. *Bulletin of the Seismological Society of America*, Vol. 98, N. 5, p.p. 2876-2892.